HHS Public Access

Author manuscript

Biomaterials. Author manuscript; available in PMC 2018 March 27.

Published in final edited form as:

Biomaterials. 2017 May ; 125: 38–53. doi:10.1016/j.biomaterials.2017.02.016.

Subconjunctival injectable dendrimer-dexamethasone gel for the treatment of corneal inflammation

Uri Soiberman[a,b,1], **Siva P. Kambhampati**[a,1], **Tony Wu**[a,c], **Manoj K. Mishra**[a], **Yumin Oh**[a], **Rishi Sharma**[a], **Jiangxia Wang**[e], **Abdul Elah Al Towerki**[d], **Samuel Yiu**[a,b], **Walter J. Stark**[a,b,**], and **Rangaramanujam M. Kannan**[a,*]

[a]Center for Nanomedicine, Wilmer Eye Institute, Department of Ophthalmology, Johns Hopkins University School of Medicine, Baltimore, MD, USA

[b]Cornea Division, Wilmer Eye Institute, Johns Hopkins University School of Medicine, Baltimore, MD, USA

[c]Department of Biomedical Engineering, Johns Hopkins University, Baltimore, MD, USA

[d]King Khaled Eye Specialist Hospital, Riyadh, Saudi Arabia

[e]Department of Biostatistics, Johns Hopkins University Bloomberg School of Public Health, Baltimore, MD, USA

Abstract

Corneal inflammation is often encountered as a key pathological event in many corneal diseases. Current treatments involve topical corticosteroids which require frequent instillations due to rapid tear turnover, causing side-effects such as corneal toxicity and elevated intraocular pressure (IOP). Hence, new interventions that can reduce side effects, dosing frequency, and increase patient compliance can be highly beneficial. In this study, we explore a subconjunctival injectable gel based on G4-PAMAM dendrimer and hyaluronic acid, cross-linked using thiol-ene click chemistry, incorporated with dendrimer dexamethasone (D-Dex) conjugates as a potential strategy for sustained delivery and enhanced bioavailability of corticosteroids. The efficacy of the injectable gel formulation was evaluated in a rat mild alkali burn model. Fluorescently-labelled dendrimers (D-Cy5) incorporated in the gel release D-Cy5 *in vivo*. The released D-Cy5 selectively targets and localizes within corneal macrophages in inflamed rat cornea but not in healthy controls. This pathology dependent biodistribution was exploited for drug delivery, by incorporating D-Dex in the injectable gel. The attenuation of corneal inflammation by D-Dex gels was assessed using various clinical and biochemical parameters over a 2-week period. Subconjunctival D-Dex gel treatment resulted in favorable clinically-relevant outcomes with reduced central corneal thickness and improved corneal clarity compared to free-Dex and placebo gel controls. The extent of corneal neovascularization was significantly reduced in the D-Dex group. These findings suggest that D-Dex attenuates corneal inflammation more effectively than free-Dex by attenuating macrophage infiltration and pro-inflammatory cytokines expression. A

*Corresponding author. Center for Nanomedicine at the Wilmer Eye Institute, 400 North Broadway, Baltimore, MD 21231, USA, krangar1@jhmi.edu, (R.M. Kannan). **Corresponding author. Wilmer Eye Institute, Center for Nanomedicine at the Wilmer Eye Institute, 600 North Wolfe Street, Baltimore, MD 21287, USA. wstark@jhmi.edu (W.J. Stark).

[1]Co-first authors with equal contribution to this work.

significant elevation in IOP was not observed in the D-Dex group but was observed in the free-Dex group. This novel injectable D-Dex gel may be a potential drug delivery platform for the treatment of many inflammatory ocular surface disorders such as dry eye, autoimmune keratitis and post-surnical complications where frequent steroid administration is required.

Keywords

Corneal inflammation; Macrophages; Dendrimers; Dexamethasone; Hyaluronic acid; Injectable gel

1. Introduction

Corneal inflammation remains a major and common clinical problem underlying many disease processes, such as: severe dry eye, infectious keratitis, chemical burn related injuries, corneal graft rejection and others [1–6]. If left untreated at its initial stages, corneal inflammation often progresses to a chronic stage and this persistent infiltration of the cornea by white blood cells and macrophages may lead to neovascularization, corneal opacity, edema, and vision loss [7,8]. So, a timely treatment of inflammation in the cornea is highly beneficial.

The standard of care for corneal inflammation is the topical administration of corticosteroids and this treatment paradigm has not changed significantly over the past few decades [9]. Many commercially available steroid eye drops, such as dexamethasone and prednisolone show potent anti-inflammatory effects [10,11]. However, due to the rapid tear turnover and clearance of the instilled drugs, repeated instillations are often required which results in patient incompliance particularly in elderly [11–14]. In addition, steroids are often associated with an increase in intraocular pressure (IOP) and the development of cataracts [15]. A clinically significant increase in IOP may require the use of antihypertensive eye drops which by themselves cause ocular surface toxicity [16]. Periocular administration of corticosteroids using the subconjunctival route as a depot can be an attractive alternative as it leads to high local drug levels that are necessary to alleviate postoperative inflammation, especially in the setting of a corneal transplant [17–19]. Several studies have reported better clinical outcomes, such as reduction in neovascularization, preservation of corneal clarity and reduction of inflammation, with subconjunctival depot injections of steroids [17,18,20–23]. A single subconjunctival corticosteroid administration results in higher drug concentration than several topical administrations [17,24,25]. However, an increase in IOP and rapid clearance of steroids is also a concern, irrespective of the route of administration [17]. Hence, developing a sustained steroid delivery system to the anterior segment is highly desirable.

Polyamidoamine (PAMAM) dendrimers are hyperbranched polymeric nanocarriers. They possess many favorable properties that make them excellent ocular drug delivery systems: they are nano-sized, multivalent, monodisperse and highly water-soluble particles [11,26]. Hydroxyl-terminated PAMAM dendrimers (G4-OH) due to their improved safety profile and near neutral surface charge significantly reduce non-specific retention and interactions in the tissues [27]. The multiple hydroxyl groups present on the surface can be easily manipulated

for introducing drugs, imaging agents or for complexing biologics [11,28–31]. Dendrimer-triamcinolone acetonide (D-TA) conjugates enhances drug solubility and intracellular delivery of TA resulting in improved antiangiogenic and anti-inflammatory activity [32]. Single intravitreal injection of dendrimer-fluocinolone acetonide conjugates attenuates neuroinflammation and provides sufficient neuroprotection for more than 30 days in rat model of retinitis pigmentosa at a 30-fold lower dose than free drug [33]. Upon systemic administration dendrimers selectively target, localize and remain in activated microglia/macrophages in the retina and brain in ischemia/reper-fusion (I/R) injury mice, cerebral palsy (CP) rabbit model and canine model of hypothermic cardiac arrest [34–36]. When delivered topically, dendrimer-encapsulated with anti-glaucoma drugs resulted in higher concentrations of drugs in corneal layers with better efficacy compared to regular eye drops, suggesting they improve tissue permeability of drugs [37].

Subconjunctival injectable hydrogels can be a suitable option for sustained delivery and improving the bioavailability of steroids thereby avoiding frequent injections [38,39]. Additionally, targeting steroids to the inflammatory cell will be highly beneficial and may improve drug efficacy and reduce side effects. In this study, we designed an injectable and biocompatible hydrogel based on hydroxyl-terminated PAMAM dendrimers and hyaluronic acid cross-linked via thiol-ene click chemistry for subconjunctival injections. This injectable gel system can easily be loaded in to applicable syringes as solutions and can be crosslinked upon UV treatment. We further synthesized dendrimer dexamethasone (D-Dex) conjugates and incorporated them in injectable gel formulation. We hypothesize that sustained release of D-Dex from the injectable gel and the targeting ability of dendrimers to inflammation associated cells will lead to a synergistic effect and that D-Dex will be have a better anti-inflammatory effect than a free drug (dexamethasone). In this study we used a rat corneal mild alkali burn model in order to demonstrate the macrophage targeting ability of dendrimer conjugates released from an injectable gel; and to attenuate corneal inflammation. The evaluation included a combination of clinically-relevant and biochemical parameters.

2. Materials and methods

2.1. Chemicals and reagents

Hydroxyl-functionalized ethylenediamine core generation four PAMAM dendrimers (G4-OH; diagnostic grade; 64 endgroups) were purchased from Dendritech Inc. (Midland, MI, USA). Dexamethasone (Dex), Succinic anhydride (SA), *N,N'*-diisopropylethylamine (DIEA), trifluoroacetic acid (TFA), anhydrous dimethylformamide (DMF), dimethylacetamide (DMA), 3-(Tritylthio)propionic acid and 4-Pentenoic acid (Kosher) were purchased from Sigma-Aldrich (St. Louis, MO, USA). (Benzotriazol-1-yloxy)tripyrrolidino-phosphonium hexafluorophosphate (PyBOP) was purchased from Bachem Americas Inc. (Torrance, CA, USA). Cy5-mono-NHS ester was purchased from Amersham Biosciences-GE Healthcare (Pittsburgh, PA, USA). Dexamethasone 21-phosphate disodium salt was purchased from MP biomedicals (Santa Ana, CA, USA). ACS grade DMF, dichloromethane (DCM), diethylether, hexane, ethyl acetate, HPLC grade water, acetonitrile, and methanol were obtained from Fisher Scientific and used as received for dialysis, purification and

column chromatography. Dialysis membrane (MW cut-off 1000 & 2000 Da) was obtained from Spectrum Laboratories Inc. (Rancho Dominguez, CA, USA).

The reactions were carried out under nitrogen. Thin-layer chromatography (TLC) was performed on silica gel GF_{254} plates (Whatman, Piscataway, NJ), and the spots were visualized with UV light. Proton NMR spectra of the final conjugates as well as intermediates were recorded on a Bruker (500 MHz) spectrometer using commercially available DMSO-d_6 solvent. Proton chemical shifts were reported in ppm (δ) and tetramethylsilane (TMS) used as internal standard. All data were processed using ACD/NMR processor software (Academic Edition).

2.2. Synthesis of dendrimer conjugates

2.2.1. Synthesis of dexamethasone-21-succinate (Dex-linker, 1)—

Dexamethasone-21-succinate (Dex-linker, *1*) was synthesized using a modified synthesis procedure established previously [32]. A detailed synthesis description is provided as a part of supplementary information (S.1).

2.2.2. Synthesis of dendrimer-dexamethasone conjugates (D-Dex, 2)—

Dexamethasone-21-succinate (Dex-linker, 255 mg, 0.541 mmol) was dissolved in anhydrous DMF (5 mL) in a 50 mL round bottomed flask under nitrogen at 0 °C to which PyBOP (703.9 mg, 1.35 mmol) dissolved in DMF (5 mL) and DIEA (300 μL) were added. The reaction mixture was allowed to stir for 1 h in an ice bath. PAMAM G4-OH (505 mg, 0.036 mmol) dissolved in anhydrous DMF (10 mL) was added dropwise to the reaction mixture above and stirred for 48 h under nitrogen. The solvent mixture was evaporated at 25 °C under vacuum. The crude product was re-dissolved in DMF (20 mL) and subjected to dialysis in DMF (membrane MW cutoff = 2 kDa) for 48 h, the DMF was evaporated under reduced pressure and D-Dex is subjected to water dialysis to remove solvent traces. The resultant water layer was lyophilized to get a fluffy white powder of D-Dex conjugate (600 mg) (Fig. 1). The formation of D-Dex conjugates were characterized using ^{1}H NMR.

2.2.3. Characterization of dendrimer drug conjugates—

The synthesized dendrimer drug conjugates were characterized using high performance liquid chromatography (HPLC), dynamic light scattering (DLS) and zeta potential, and matrix assisted laser desorption/ ionization (MALDI-TOF). The drug release was evaluated in simulated tear fluid (STF). The detailed procedures are described as the part of supplementary information (S.2).

2.2.4. In vitro evaluation of dendrimer dexamethasone conjugates—

In vitro cytotoxicity and anti-inflammatory activity of dendrimer dexamethasone conjugates were evaluated in a murine macrophage (RAW 264.7) cell line. A detailed procedure is described as the part of supplementary information (S.3).

2.3. Synthesis of individual components of the injectable gel

2.3.1. Synthesis of dendrimer-4-pentenoic acid conjugates (D-Ene, 7)—

The detailed synthesis procedure for dendrimer-4-pentenoic acid conjugates (D-Ene, 7) is provided as a part of the supplementary information (S.4).

2.3.2. Synthesis of thiolated hyaluronic acid (HA-SH, 6)—Prior to the synthesis of HA-SH, sodium salt of hyaluronic acid (HA) was converted to tetrabutylammoninum salt (HA-TBA), so that it could be solubilized in DMSO/DMF (20:80) for efficient thiolation reaction. To make HA-TBA, hyaluronic acid was dissolved in ultrapure DI water at 2% (w/w) and the ion exchange was done by adding Dowex 50 W proton exchange resin (3 g resin per 1 g HA) with vigorous stirring for 5 h. The resin was filtered off using Whatman filter paper and the filtrate was titrated to a pH of 7.4 with tetrabutylammoninum-hydroxide TBA-OH. The product was lyophilized at −80 °C to obtain an off-white floppy solid material that was then dissolved in DI-H_2O and subjected to water dialysis (membrane MWCO = 2 kDa) to remove excess TBA-OH. The resultant water layer was then subjected to lyophilization and stored at −20 °C until used. The ion exchange was confirmed using ^{1}H NMR analysis.

HA-TBA (680 mg, 0.027 mmol) was dissolved in 10 mL of anhydrous DMSO at 50 °C under nitrogen atmosphere, to which DCC (640 mg, 3.01 mmol) and DMAP (137.5 mg, 1.12 mmol) dissolved in 10 mL of anhydrous DMF were added. 3-(Tritylthio) propionic acid (348 mg, 2.2 mmol) was dissolved in 10 mL of anhydrous DMF and added dropwise into RBF and the reaction was stirred for 48 h under nitrogen atmosphere at room temperature. The reaction mixture was then centrifuged to remove formed DCU and the solvent layer was dialyzed against DMF in 8 kDa MWCO dialysis tubing for 36 h to remove impurities. The solvent was evaporated and the compound was dissolved in DI water to get a milky white solution. The solution was subjected to water dialysis in 8 kDa MWCO dialysis bag for 24 h and the solution subjected to lyophilization to obtain fluffy white solid of TBA-HA-STrt (780 mg). The formation of the product was confirmed using ^{1}H NMR analysis. For trityl group deprotection TBA-HA-STrt was dissolved in DMF/DCM mixture (1:5) followed by addition of 5% TFA in the presence of Et_3SiH as a cation scavenger [40] and DTT to avoid disulfide formation. The solvent was quickly evaporated under reduced pressure to obtain sticky semi-solid TBA-HA-SH. The solid was washed with DCM 5 times and dissolved in NaCl solution (0.5 gm NaCl per 100 mL of H_2O with catalytic amount of DTT) and stirred for 10 min. The solution was precipitated with cold acetone thrice; then with cold ethanol five times to remove DTT and excess salt. The product, a white solid material, was dissolved in DI water and immediately subjected to liquid nitrogen and lyophilized to obtain white powder of HA-SH (370 mg). The final product (HA-SH, **6**) was confirmed using ^{1}H NMR analysis.

2.4. Preparation of injectable D-Dex gel for efficacy studies

Injectable D-Dex gel was prepared via thiol-ene photo-polymerization by using the dendrimer component (D-Ene) and the hyaluronic acid component (HA-SH) in the ratio of 1:2 respectively. Briefly, 2% solutions of individual components were prepared in PBS and stored on ice until mixed. D-Dex and free-Dex solutions were prepared by dissolving D-Dex and free-Dex (Dexamethsone-21-phosphate disodium salt), respectively, in PBS such that 10 μL of the solution contained 1.6 mg of dexamethasone. For each injection 20 μL of HA-SH solution, 10 μL of D-Ene solution, 10 μL of D-Dex or free-Dexamethasone solution and 5 μL of photo-initiator (Irgacure 2959 (Ciba, Basel, Switzerland), 5 mg/mL in DMSO) were mixed in 0.5 mL Eppendorf tubes. The hazy mixture solution was loaded onto 0.5 cc insulin

syringe and placed under UV light for 2 min. The formation of gel was confirmed by pushing the piston which released a jelly-like solution from the needle tip. (Fig. S6).

2.5. Characterization of injectable hydrogels

2.5.1. Morphology analysis of injectable hydrogels—Scanning electron microscopy (SEM) analyses were performed to investigate the surface morphology of the hydrogels. The gel pellets were fixed in 2.5% glutaraldehyde, stained with 1% osmium tetroxide, dehydrated using ethanol gradient, and desiccated with hexamethyldisilazane (HMDS). The samples were mounted on carbon stubs, sputtered with gold and imaged under Zeiss Leo FESEM at 1 kV. In order to analyze the internal structure of the hydrogels, pore size and crosslinking density, the gel pellets were fixed in 2.5% glutaraldehyde in 10% sucrose and the sucrose gradient was increased to 30%. The gels were embedded in Optimum Cutting Temperature (OCT) media (Tissue-Tek, CA, USA) and 30% sucrose (1:1) and frozen at −80 °C until they were sectioned. Gel sections (30 μm) were cut using a cryostat and imaged under Zeiss confocal 710 microscopes.

2.5.2. Rheological analysis of injectable hydrogels—Rheological experiments were carried out on a horizontal rheometer (AR20000, TA instruments, USA) using the parallel plates (25 mm, diameter) with controlled hydrated atmosphere at 37 °C in the oscillatory shear mode. Real time gelling was accessed by loading polymer solution (HA-SH +D-Ene +PI) between the plates. A strain controlled (1.0%) time sweep was conducted. At 60 s, UV light was illuminated and the crosslinking was accessed for their viscoelastic properties. To study the viscoelastic behavior and dynamic viscosity of the injectable gels, pre-cured gel solution (300 μL) was loaded between the plates and a frequency sweep was performed which covered a range of frequencies from 0.01 to 10 Hz at a controlled regular strain of 1.0% (within linear viscoelastic range (LVER) 0.5–2%). The storage modulus G', loss modulus G'' and dynamic viscosity η were obtained as a function of shear frequency.

2.5.3. Swelling, degradation and release studies of D-Dex or free-Dexamethasone from gel formulations—Swelling and degradation of the injectable gel were assessed in phosphate buffer saline (PBS 1X, pH 7.4) and citrate buffer (pH 5). For stability studies gel pellets with known amount of D-Dex or free-Dex were made using the circular crevice in the caps of the 2 mL Eppendorf tubes (diameter = 8.0 mm and thickness 4 mm). The pre-weighed pellets (n = 3, for each group) were placed in 12 well plates containing 1 mL of buffer and incubated at 37 °C. At particular time points the pellets were carefully lifted using a spatula and the excess moisture was blotted out using Kim wipes and weighed. The swelling ratio was calculated using the equation (W_c/Wi) X 100, where W_c is the current swollen weight and W_i is the initial weight of the gel. In order to measure degradation rates, the gel pellets were placed in 2 mL Eppendorf tubes and preweighed. The tubes were then filled with 1.5 mL of buffer (either pH 5.0 or pH 7.4) and incubated at 37 °C on a test tube rocker. At particular time points the contents of the individual tubes were centrifuged at 2000 rpm for 5 min and the buffer was carefully removed. The gel pellets along with the tubes were lyophilized and the weight changes were noted. The release of D-Dex and free-Dex from the injectable gel was analyzed by incubating the gel pellets in 8 mL scintillation vials containing 5 mL of buffer solution. At particular time points 200 μL of

samples were withdrawn and injected into HPLC using the same method as mentioned in HPLC section. The percent of released Free-Dex from D-Dex was quantified using a calibration graph.

2.6. Animals and corneal alkali burn model

All procedures involving animals conformed to the Association for Research in Vision and Ophthalmology Statement for the use of Animals in Ophthalmic and Vision Research and the study procedures were approved by the Johns Hopkins University Animal Care and Use Committee. Thirty-five Lewis rats (7–8 weeks of age) were obtained from Harlan Laboratories Inc. (Frederick, MD, USA). All animals weighed between 150 and 200 g and were housed at constant temperature (20 ± 1 °C) and humidity (50± 5%). They were fed standard rat chow and allowed water *ad libitum*. All procedures and tests were performed under general anesthesia with intramuscular injection of ketamine 0.9% (Bio-niche Pharma, Lake Forest, IL, USA), xylazine 0.1% (Phoenix Pharmaceuticals, St. Joseph, MO, USA) and topical proparacaine 0.5% (Sandoz, Holzkirchen, Germany). Corneal alkali burns were induced by application of 0.5 N NaOH on the cornea. Briefly, sample discs SS-033, 0.5 cm in diameter (WESCOR, Logan, Utah, USA) were cut into 4 quadrants that were then soaked in 0.5 N NaOH for 10 s and then placed on central cornea for 15 s. The ocular surface and conjunctival fornices were immediately irrigated with 15 mL of PBS solution using an eye-drops dropper bottle.

2.7. Qualitative biodistribution studies, immunohistochemistry and confocal microscopy

For biodistribution studies, we used fluorescently labelled G4-OH dendrimers (D-Cy5) in order to allow particle visualization using a confocal microscope. The synthesis and characterization of D-Cy5 were previously published by our group [34,35]. Briefly, D-Cy5 was dissolved in PBS (250 μg D-Cy5 in 10 μL) and integrated into 40 μL of an injectable gel system. It was then loaded into 0.5 mL 30G insulin syringes and exposed to UV light for 3 min until a gel was formed. The D-Cy5 gels were injected into the subconjunctival space. This led to the formation of blebs. The rats were euthanized in a CO_2 chamber seven days after the injection of D-Cy5. The eyes were enucleated and washed in ice cold PBS for 5 min. The eyeballs were then fixed in 4% PFA in 5% sucrose solution for 5 h and then subjected to treatment with sucrose gradient as previously described [41]. The eyeballs were frozen in a 20% Sucrose/OCT medium in a 1:2 ratios, respectively, using dry ice in isopentane. Cryoblocks were sectioned (20 μm thickness) using a cryostat (Microm, Walldorf, Germany). Four sections from each cryoblock were used for image analysis. The sections were incubated in rabbit anti-ionized calcium binding adapter 1 molecule (Iba-1; Wako Chemicals, Richmond, VA, USA), which is a macrophage cell marker. The samples were then incubated in a goat anti-rabbit-Cy3 secondary antibody solution (Life Technologies, Grand Island, NY, USA) and in isolectin GS-IB4 AF488 (Thermo Fisher, MA) that was used as a marker for corneal stroma and blood vessels. The sections were analyzed using a confocal microscope (model 710 unit; Carl Zeiss, Inc., Thornwood, NY, USA). Excitation and emission wavelengths and laser settings were identical for all tissues. Z-stacks of sections were taken and collapsed to give an image through the depth of the whole section.

2.8. Subconjunctival treatment and efficacy of D-Dex gel and Free-Dex gel

After alkali burn, the animals were randomized to be treated with Dendrimer-dexamethasone conjugates (D-Dex group, n = 10), free-Dexamethasone (Dexamethsone-21-phosphate disodium salt) (free-Dex group, n = 10) in injectable gel formulation or no drug (only injectable gel, n = 10). The latter served as positive placebo gel controls. Both D-Dex and free-Dex groups were treated with a nearly identical dosage of dexamethasone (1.6 mg/eye) present in both D-Dex and free-Dex formulations (1.76 mg of dexamethasone for the D-Dex group and 1.6 mg for the free-Dex group). The reason for this minimal and clinically insignificant discrepancy in doses was that drug release studies demonstrated that the dexamethasone dose released by the D-Dex conjugates in the first days was inadequate to control inflammation. Clinically, it is important to control inflammation at its onset, so a decision was made to augment D-Dex with a bolus of 10% free dexamethasone per eye. This minimal added dose is highly unlikely to account for any clinical differences observed between groups. All study drugs were incorporated into injectable gel formulations and injected subconjuntivally using 30G, 0.5 cc insulin syringes and the total volume did not exceed 40 μl.

2.9. Clinically-relevant evaluation of D-Dex and Free-Dex injectable gels treatment efficacy

Animals were assessed at baseline and at the following postexposure time points: 24 h, 72 h, and 7 days. A subset of the animals was also followed up to 14 days. The assessed parameters included the following:

2.9.1. Optical coherence tomography (OCT)—The central corneal thickness was evaluated using anterior segment optical coherence tomography (Bioptigen, NC, USA).

2.9.2. Intraocular pressure measurements—The intraocular pressure was measured using a handheld tonometer (iLab tonometer, iCare, Finland). The setting R for rat was chosen and the tonometer was used according to the manufacturer's instructions.

2.9.3. Corneal opacity and neovascularization scores by clinical observation—The corneal opacity was scored by grading the degree of transparency (Table 1) as previously described by *Larkin D.F.* et al. [42]. The estimated area of neovascularization (NV) was assessed by estimating the radial penetration of the neovascular vessels and their extent in degrees using an ophthalmic operating microscope, and by assuming a mean rat corneal diameter of 2.5 mm, so that the maximal area of NV was no more than $2.5^2\pi$ mm^2 (=19.63 mm^2).

2.10. Biochemical evaluation of D-Dex and Free-Dex efficacy

At the end of the follow-up period (day 7 and day 14), the animals were euthanized using a CO_2 chamber and the corneas were excised and processed for either immunohistochemistry (n = 3, for each group) or frozen in liquid nitrogen for RNA extraction for RT-PCR studies (n = 10, for each group).

2.10.1. Immunohistochemistry—Upon removal, the corneas were prepared for immunohistochemistry studies as explained in section 3.1. The stained sections were imaged under a confocal microscope.

2.10.2. RNA extraction and RT-PCR studies for cytokine expression—The corneas were snap frozen in liquid nitrogen and homogenized carefully into tissue powder using pre-frozen (in liquid nitrogen) porcelain mortar and pestles. Total RNA was purified from this frozen powder with TRIzol reagent (Life Technologies, Grand Island, NY) according to the manufacturer's instruction. 3 μg of total RNA was reverse-transcribed to cDNA using high-capacity cDNA reverse transcription system (Life Technologies) according to the manufacturer's instructions. qRT-PCR was performed with fastSYBR Green Master Mix (Life Technologies) by a StepOnePlus Real-Time PCR System (Life Technologies). The primers for the following cytokines were used for amplification: TNF-α, IL-1β, MCP-1, IL-6 and VEGF (see Table 2 for primer sequences). The expression of rat GAPDH mRNA was used to normalize the expression levels of target genes and was calculated by the comparative cycle threshold Ct method ($2^{-\Delta\Delta Ct}$).

2.11. Statistical analysis

For corneal thickness and intraocular pressure, mixed effects regression models were employed for the between group comparisons for the D-Dex, free-Dex, and positive controls, and the within group comparisons between post-operative days for each group. The models include an interaction terms between the groups and the days the measures were taken, and a random intercept for eyes to account for the correlation among the repeated measures from the same eye. Due to the discrete distribution of opacity scores, within group comparisons between post-operative days are from Wilcoxon signed-rank test, and the between group comparisons are from two-sample Wilcoxon rank-sum (Mann-Whitney) tests. Data were analyzed using statistical software, Stata, version 13, software (College Station, TX). P values less than or equal to 0.05 are considered statistically significant. For PCR analysis, given the large number of comparisons, a Bonfferoni correction was employed and a p value less than or equal to 0.001 were considered statistically significant. Eyes with corneal perforation were excluded from the analysis of CCT – this finding was seen only in the free-Dex group.

3. Results and discussions

3.1. Synthesis of Dex-linker and D-Dex conjugates

Dendrimer-dexamethasone conjugates (D-Dex) were prepared using a two-step synthesis procedure as shown in Fig. 1, and were characterized using ^{1}H NMR and HPLC. In the first step, Dexamethasone was functionalized with a carboxylic acid terminal group using succinic anhydride dissolved in DMA/DMF mixture in the presence of triethylamine to get Dexamethasone-21-succinate (Dex-linker, ***1***). Dexamethasone has three hydroxyl groups and the most reactive hydroxyl group is at the 21-position. We avoided the conjugation of linker to –OH groups at 11 and 17 positions of dexamethasone by using no more than 1.2 mol equivalents of succinic anhydride in the reaction. Dex-linker was further purified using column chromatography to remove unreacted reagents. The structure of Dex-linker was

established by ^{1}H NMR spectra, and characteristic peaks at 1.77, 2.33 and 2.48 ppm correspond to –CH_2 protons of linker; a peak at 12.25 ppm that correspond to carboxylic acid confirmed the formation of Dex-linker (Fig. S1). The Dex-linker was further conjugated with PAMAM dendrimer (G4-OH) using PyBOP as coupling and DIEA as base to produce the therapeutic conjugate, D-Dex (2). As shown by ^{1}H NMR spectrum, three peaks at 0.80, 0.88 and 1.49 ppm represent methyl protons (–CH_3) of dexamethasone. Moreover, the appearance of a new peak at 4.02 ppm corresponds to modified methylene protons of dendrimer whereas peaks between 5.0 and 7.4 ppm correspond to the aromatic protons of dexamethasone). Together, these NMR findings confirm the formation of D-Dex conjugates (Fig. S2). Moreover, using NMR proton integration technique, we estimated that ~9–10 molecules of dexamethasone were conjugated to one dendrimer molecule. The conjugates were readily soluble in water, PBS buffer, and saline.

3.2. Physicochemical characterization of D-Dex conjugates

The purity of the conjugate and the Dex-linker were determined using reverse phase HPLC. The hydrophobic free-Dex eluted at 22.4 min, whereas the Dex-linker eluted at 27.6 min. At similar HPLC conditions, a broad peak at 32.8 min was observed for D-Dex conjugate (monitored at 240 nm) which is different from that for the starting dendrimer (retention time 15 min) suggests successful conjugation of Dex to dendrimer surface. The conjugate is pure since we did not observe any ‘characteristic’ peaks related to free-Dex and Dex-linker (Fig. 2A). MALDI-TOF analysis of unmodified G4-OH dendrimer gave a peak at 41.1 kDA and after conjugating Dex resulted in a shift in mass peak to 18.3 kDa suggesting that ~9 molecules of Dex attached to the dendrimer and agreeable with the ^{1}H NMR characterization. The size and surface charge of G4-OH dendrimers (D) was 4.4 ± 0.2 nm and 4.5 ± 0.2 mV respectively. Upon conjugating ~9 molecules of Dex to the dendrimer, there was a small increase in size (5.6 ± 0.4 nm) and slight increase in zeta potential (5.3 ± 0.2 mV). DLS and zeta experiments suggests that upon conjugating 9–10 molecules of dexamethasone on to dendrimer may not significantly alter the cellular entry or biodistribution in tissues.

3.3. Release study of D-Dex conjugates

We used HPLC to quantify the release characteristics of the D-Dex conjugate. The specifically designed D-Dex conjugate had two ester-linkages between the dendrimers and the drug; and was therefore susceptible to hydrolysis. In order to emulate the environment of the ocular surface, that includes the cornea and conjunctival sac, the chosen aqueous solution was simulated tear fluid (STF). Ocular surface inflammation induces a change in the pH of the tear film – it increases to 7.5 [43] so we used STF with an identical pH. D-Dex conjugates released the drug as either dexamethasone or Dex-linker. In STF, the D-Dex conjugates released the drug in a sustained fashion over weeks. At earlier time points, D-Dex conjugates released the drug more in the form of Dex-linker than as free Dex. At the 24 h time point, there was minimal release of ~5.2% of Dex (free Dex- ~0.2% and Dex-linker- ~5%) (Fig. 2B). At 7 days, the conjugate released ~27.8% of the drug (~18.7% Dex-linker and ~9.1% free Dex). Subsequently, from day 7 till day 15, we observed a cumulative release of ~55.8% (~50% free Dex and ~5.8% Dex-linker). Interestingly, the area corresponding to the Dex-linker decreased and that of free Dex increased suggesting that the

ester bond between the linker and the steroid is mostly stable for a period of 7 days, but is cleaved afterwards, as observed by Macky et al. [44]. From day 15 to day 25, we observed near zero order release, with a cumulative release of ~75% of the payload (Fig. 2B). After 40 days, conjugates released ~95% of its payload, suggesting that the conjugate can deliver drugs in a sustained fashion in STF. There are two ester bonds in D-Dex conjugates (i) an ester bond between the dendrimer surface and the Dex-linker and (ii) another ester bond between the linker and Dex. The possible mechanism for Dex release can be attributed to hydrolysis of aforementioned ester linkages in aqueous conditions of STF. Even though D-Dex releases Dex more in the form of Dex-linker rather than free Dex at early times, we expect that this type of release will not affect the therapeutic activity of dexamethasone because the hydroxyl group at 21st position used in the conjugation is not required for any therapeutic activity or receptor binding [9,10].

3.4. In vitro efficacy of D-Dex conjugates

We evaluated the cytotoxicity profile of D-Dex conjugate in the RAW 264.7 cell line derived from murine macrophages as macrophages are the target for D-Dex in this study. We observed that free-Dex at 200 μg/mL exhibited ~30.2% ± 3.4% reduction in cell viability whereas D-Dex (containing equivalent of Dex in conjugated form) was less cytotoxic (~14.9% ± 2.7% reduction in cell viability). At concentrations below 100 μg/mL, the cell viability was >90% for both free-Dex and D-Dex (Figure S3A).

The anti-inflammatory activity of D-Dex conjugates was evaluated in lipopolysaccharides (LPS) activated pro-inflammatory macrophages. A 3-h treatment of RAW 264.7 cells with 100 ng/mL of LPS resulted in the increased production of tumor necrosis factor (TNF-α) for 48 h. We used TNF-α suppression to evaluate the anti-inflammatory properties of D-Dex. LPS activation resulted in an increase (~2.5 fold) in TNF-α levels. The cells were exposed to D-Dex, free-Dex and Dex-linker for 12 h. Therefore, the antiinflammatory effect reflects the uptake and release of the drug inside cells over a 12 h period. The medium was removed at 12 h, and replaced with LPS medium for 24 h. D-Dex demonstrated dose dependent activity in suppressing TNF-α production by LPS activated cells. At 100 μg/mL D-Dex demonstrated enhanced antiinflammatory activity by inhibiting TNF-α (~56% decrease) compared to LPS activated cells, free-Dex and Dex linker (Figure S3B). Both free-Dex and Dex-linker demonstrated similar TNF-α suppression (~24% and ~21% decrease respectively). So, conjugating a succinic acid linker to dexamethasone did not reduce anti-inflammatory activity of dexamethasone. At low concentrations (10 μg and 1 μg/mL), D-Dex demonstrated significant suppression of TNF-α (~52% and 60% respectively), whereas free-Dex and Dex linker did not demonstrate any anti-inflammatory activity (Figure S3B). This also suggests enhanced intracellular uptake of D-Dex by macrophages as observed previously by our group [32].

3.5. Synthesis of individual components of the injectable gel

Dendrimer-pentenoic acid conjugates were synthesized using single step coupling reactions between surface hydroxyl groups (–OH) of PAMAM dendrimers and the carboxylate moiety of 4-pentenoic acid. This was achieved using PyBOP as a coupling agent and in the presence of DIEA as base under nitrogen atmosphere [Fig. 1B(ii)]. In the ^{1}H NMR spectrum of D-

Ene conjugate, appearance of two new multiplets at 4.96–5.05 ppm and 5.77–5.82 ppm corresponds to H_2C = and = CHC alkene protons of 4-pentenoic acid. Further, appearance of a new peak at 4.00 ppm [corresponding to modified methylene protons (–CH_2) of dendrimer] suggests that 4-pentenoic acid was successfully conjugated to the dendrimer (Fig. S4). Using NMR proton integration technique, we estimated that approximately 28–29 molecules of 4-pentenoic acid were conjugated to one dendrimer molecule. The conjugates were readily soluble in water, PBS buffer and saline.

Thiolation of hyaluronic acid (HA-SH) has been reported previously by many research groups [45–48]. *Kafedjiiski* et al. [45] have reported a facile method for the synthesis of thiolated hyaluronic acid by conjugating *L*-cysteine ethyl ester to the hyaluronic acid using an aqueous solvent; the resultant product was subjected to oxidation to form disulfide (–S–S–) bridges allowing HA to form gels for drug delivery. In this study, we intend to have free thiols on hyaluronic acid to facilitate thiol-ene clickable polymerization reaction for injectable gels. Since the aforementioned reaction was performed in aqueous medium which may result in *in-situ* disulfide formation. In this study, we adopted an alternative method for synthesis by modifying HA to enable reactions under inert conditions as reported previously [49,50]. HA-SH was synthesized using a three-step process as shown in Fig. 1 B(i). In the first step the commercially available sodium salt of hyaluronic acid (HA) was converted to DMF/DMSO soluble tetrabutylammoninum (TBA) salt (HA-TBA) using the ion exchange method. The exchange of Na^+ by TBA^+ ions were confirmed using ^{1}H NMR analysis showing appearance of new peaks between 3.21 and 0.93 ppm (–CH_3, t) at 0.94 ppm, (–CH_2, dd) at 1.36 ppm, (–CH_2, m) 1.66–1.63 ppm, and (–CH_2, m) 3.21–3.18 ppm (Fig. S5B). In the second step, 3-(tritylthio)propionic acid was conjugated to the hydroxyl (–OH) groups of hyaluronic acid using a Steglich esterification reaction. We used trityl protected thiopropionic acid to avoid thioester and disulfide bonds formation. ^{1}H NMR analysis demonstrated the appearance of new peaks (–CH_2, t) at 2.33 ppm and 2.49 ppm which corresponds to methylene (–CH_2) protons of propionic acid. New multiplet peaks between 7.45 and 7.20 ppm correspond to trityl protons. Added together, these findings confirm the formation of TBA-HA-STrt (Fig. S5C). In the third step, we selectively deprotected the trityl group using 5% TFA in a DMF/DCM (1:5) mixture and in the presence of Et_3SiH to obtain a TBA-HA-SH intermediate. Then, TBA^+ groups were fully exchanged using NaCl solution and the reaction mixture was washed with cold acetone and ethanol to remove the excess TBA, DTT and NaCl to yield hyaluronic acid bearing free –SH end groups. Removal of TBA was confirmed by the absence of its characteristic peaks in ^{1}H NMR and presence of methylene (–CH_2, m) protons at 2.92–2.90 ppm and 2.10–2.08 ppm. The disappearance of multiplets corresponding to the trityl group between 7.45 and 7.20 ppm and the simultaneous appearance of a triplet at 1.20 ppm corresponding to presence of free thiol (–SH) confirms the formation of thiolated hyaluronic acid (HA-SH, ***6***) (Fig. S5D). Using proton integration method, we estimated that approximately 18–20 molecules of mercaptopropionic acid were conjugated to each hyaluronic acid polymer resulting in high degree of thiolation (~30%). HA-SH was highly soluble in aqueous solutions.

3.6. Formation and characterization of injectable gels

Injectable D-Dex eluting hydrogels were produced by crosslinking aqueous solutions of D-Ene and HA-SH using thiol-ene click chemistry in the presence of Irgacure 2959 (as a photo-initiator) and UV light (Figs. 1C and S6). D-Ene was used in order to anchor the linear thiolated hyaluronic acid (HA-SH) to form 3-dimensional cross-linked gels. Thiol-ene click chemistry was utilized for this process because it is a highly efficient free radical-mediated photopolymerization reaction and it has rapid gelation time [51–53]. Upon UV exposure (350 nm UV-A), the photo initiator was excited to generate thiyl radicals. The formed thiyl radicals propagate through ene ($=CH_2$) moieties on dendrimer resulting in additiontype polymerization, and forming soft, injectable hydrogels. A specific consistency was sought while producing this gel, as injection through a small bore needle (standard in ophthalmic care) can only be done with soft gels. Moreover, the degradation of the gel had to occur in a timely manner in order to facilitate drug delivery over time. In addition, a rigid gel may cause irritation if present underneath the conjunctiva for a prolonged period of time. So, different hydrogel formulations were evaluated by adjusting the polymer concentration (1%, 2%, and 5%) and the ratios of hyaluronic acid (HA-SH) and dendrimer (D-Ene) (1:1, 2:1, and 1:2). Optimal results were obtained with 2% polymer concentration and 2:1 ratio (HA-SH: D-Ene). Higher polymer concentrations or increasing dendrimer content in the ratio resulted in delayed polymerization and harder gels. A higher HA-SH concentration was favored during the production process of the gel is at led to the creation of a more flexible and soft gel. Hyaluronic acid (HA) has shear thinning properties with a high capacity for lubrication, water absorption and retention. It also influences several cellular mechanisms for wound healing [54]. These traits made HA-optimal for the preparation of this hydrogel. An image of the formed hydrogel is depicted in Fig. S6.

3.7. Rheological properties and morphology of injectable hydrogels

The formation of gel and crosslinking kinetics were assessed using time sweep measurements. Before UV irradiation (till ~60 s) and until 40 s after irradiation, the solution had a low viscosity (Fig. 3A), suggesting an easily injectable solution. After UV irradiation at 60 s, storage modulus (G') increased, the loss modulus (G'') stabilized, with the crossover point ($G'>G''$) occurring at ~160 s (i.e. 100 s after UV treatment), suggestive of gelation via thiol-ene click within the loaded polymer solution over this period (Fig. 3A). This suggests that gelation occurred within little ~1 min of UV exposure and the gels reached a storage modulus of ~1 kPa. The gelation time was unaffected with the incorporation of D-Dex in the prepolymer solution. The frequency sweep (0.01–10 Hz, within LVER) measurements after gelation were conducted at 37 °C under a hydrated environment, to assess G', G'' and complex viscosity ($|\eta^*|$) (Fig. 3B and C). For all injectable gels (with or without D-Dex), G'' was always lower than G' ($G'»G''$), and was independent of frequency, suggestive of a stable, viscoelastic, crosslinked network (Fig. 3B). Incorporation of D-Dex did not significantly change the rheological properties of the injectable gel (without D-Dex G'-148.4 ± 0.5 Pa, G'' – 5.2 ± 0.1 Pa, with D-Dex G' – 216.5 ± 0.9 Pa, G'' – 8.2 ± 0.08 Pa). The magnitude of the complex viscosity ($|\eta^*|$) decreased with increasing frequency, indicating that the injectable gel was shear thinning (Fig. 3C and D). The shear thinning was attributable to HA in the gel system, as observed in Healon (an injectable HA gel) [55,56].

There was a small increase (~22.5%) in viscosity in D-Dex incorporated gels suggestive of a small D-Dex induced filler effect.

SEM imaging was used to assess the surface morphology of the injectable gels with and without D-Dex. The HMDS dehydrated gels showed uniformly dense structures with striations in both conditions (with and without D-Dex) (Fig. 3F). Interestingly, in the dried form, D-Dex appears to be incorporated into the injectable gel as precipitates (Fig. 3F). Dehydration of gel samples exhibited significant reduction in volume (~45% reduction) from the hydrated state. It is likely that the removal of water causes formation of dense structure and D-Dex precipitation in D-Dex incorporated gels. The cross sections of the FITC-labelled hydrogels were imaged under confocal microscope to investigate the crosslinked morphology and pore density. The cross sections demonstrated similar crosslinked architecture forming pores with size ranging from 60 nm to 100 μm in both the naïve hydrogel and in D-Dex incorporated gel (Fig. 3G).

3.8. Swelling, degradation and release of D-Dex from injectable hydrogels

3.8.1. Swelling and degradation of injectable hydrogels—The degradation rates and swelling properties of D-Dex incorporated gel were evaluated in neutral (PBS pH 7.4) and acidic (citrate buffer pH 5.5) conditions. Under both conditions the gels exhibited similar swelling properties after 2 h of incubation with a ~25.2 ± 2.8% and ~30.1 ± 3.2% increase in weight, respectively (Fig. 2C, inset). This substantial swelling is attributed to the high water absorption and retention by HA in the gel. The gel degrades over a period of ~100 h, with no appreciable difference between the two pHs. Gel degradation may be catalyzed by hydrolysis of ester bonds in aqueous solutions. This gel formulation possesses two ester bonds: (i) an ester bond between the surface –OH group of the dendrimer and the –COOH group of pentenoic acid and (ii) an ester bond between the –OH group of hyaluronic acid and the –COOH groups of mercaptopropionic acid – both are susceptible to hydrolysis in aqueous conditions.

3.8.2. Drug release from injectable hydrogels—In order to evaluate the release of D-Dex and free Dex (Dex-phosphate) from the gel, the gel pellets were incubated in pH 7.4 and 5 buffer solutions. At various time points the solutions were sampled and the released products were analyzed using HPLC. An initial ‘fast’ release phase was observed under both conditions (pH 7.4 and pH 5). The gels released ~25% (pH 7.4) and ~37% (pH 5) of its payload over the first 10 h. During this time, the release of free Dex was faster, with ~46% in pH 7.4 and ~65% in pH 5 (Fig. 2D). This fast release can be attributed to the initial swelling of the gel. From 10 to 24 h, the gels released an additional ~10% and ~21% (for D-Dex), ~21% and ~20% (for free Dex) from initial drug loading, at pH 7.4 and 5 respectively. Within 48 h, free Dex incorporated gels released most of its payload (~95% in pH 7.4 and ~98% in pH 5) (Fig. 2D). D-Dex incorporated gels on other hand, released most of it payload over ~5 days (at pH 7.4), and over 3 days (at pH 5The slower release of D-Dex from gels may be possible due to the slower diffusion of the D-Dex conjugate (~5 nm) through the swollen gel matrix. Of note, D-Dex was released intact from the gels until 96 h (at pH 7.4), consistent with results from D-Dex release studies in STF (Fig. 2B), suggesting that D-Dex is stable at this condition. At a pH of 5, we observed an appearance of Dex-linker peak in

HPLC chromatograms from 60 h suggesting hydrolysis of ester bonds in the D-Dex conjugates at later times at lower pH. These release studies are under sink conditions, whereas *in vivo*, the amount of fluid in contact with the gel will be much lower, enabling sustained release of D-Dex over weeks from the gel, which could target inflammation.

3.9. Dendrimer biodistribution: dendrimers demonstrate pathology-dependent biodistribution

We used Iba-1 as a marker for corneal macrophages. In a normal eye, Iba-1^+ cells were found in minimal amounts in the central cornea region (Fig. 4A). Following alkali burn to the central cornea, an increase in macrophage infiltration (Iba-1^+) was noted in the corneal stroma and the epithelial layers (Fig. 4B). The burn injury also resulted in a significant increase in corneal thickness which is a finding clinically consistent with post-alkali burn keratitis (corneal inflammation). In order to demonstrate both targeting and one-week retention of dendrimers released from the subconjunctival injectable gel, we used fluorescently labelled dendrimer (D-Cy5). In order to avoid tissue auto-fluorescence we used a near IR imaging agent (Cy5) covalently attached to dendrimer using previously established procedures in our lab [34,35]. Seven days post subconjunctival injection of D-Cy5 gels, the imaging studies demonstrated pathology dependent biodistribution: D-Cy5 released from the gels were found co-localized and retained in infiltrating macrophages in the central cornea in the alkali burn group (Fig. 4B), whereas in normal eyes, no D-Cy5 signals were elicited (Fig. 4A) suggesting that dendrimer biodistribution is restricted to inflamed and pathologic tissues/cells. Additionally, alkali burn causes activation and infiltration of macrophages in the iris and D-Cy5 was also found co-localized in macrophages in the near vicinity of the iris blood vessels in inflamed tissues only (Fig. S7). The pathology dependent biodistribution can be attributed to a combination of factors such as dendrimer properties (size and surface charge), disruption of barriers in pathological tissue and altered properties of activated macrophages [27].

3.10. In vivo evaluation of anti-inflammatory activity against clinically-relevant and biochemical benchmarks

3.10.1. Clinically-relevant parameters

Central corneal thickness (CCT): There were no baseline differences in CCT between the groups (D-Dex vs. free-Dex: $p = 0.4$; D-Dex vs. positive controls: $p = 0.67$; free-Dex vs. positive controls: $p = 0.69$). CCT was increased in all groups at postoperative day (POD) POD 1 and 3 (see Figs. 5 and 6A and Table 3), as expected. By POD 7 there was a trend for improvement in corneal thickness in all groups, but it was more pronounced in the D-Dex group. Mean corneal thickness at POD14 was lowest in the D-Dex group. A comparison of the corneal thickness between the D-Dex group and the free-Dex group showed that the CCT was lower in the former at POD3 ($p = 0.04$) and POD7 ($p = 0.009$) (see Figs. 5 and 6A and Table 3). For the comparison of the D-Dex group and the positive controls, CCT was lower for the former at POD3 ($p = 0.01$), POD7 ($p = 0.001$) and POD14 ($p = 0.01$). Treatment with steroids leads to mitigation of intraocular and corneal inflammation with a resultant decrease in corneal thickness. As shown here, the D-Dex group had the most favorable outcome in terms of resolution of corneal edema following alkali burn.

Intraocular pressure: As demonstrated in Fig. 6B and in Table 3, no baseline IOP differences were found between the groups (D-Dex vs. free-Dex p = 0.25; D-Dex vs. positive controls p = 0.3; free-Dex vs. positive controls p = 0.89). Statistically significant differences were first noted at POD3: the mean IOP in the D-Dex group was 10 ± 0.2 mmHg whereas in the free-Dex group it was 12.14 ± 0.63 (p = 0.02); the mean IOP in the positive control group was 11.91 ± 1.28 (p = 0.04 for the comparison with the D-Dex group). By POD7, these differences became more apparent with the D-Dex group having a mean IOP of 11.33 ± 0.62 mmHg whereas the free-Dex group had a mean IOP of 14.45 ± 0.5 mmHg (p = 0.001). At POD14 the D-Dex group had a mean IOP of 10.9 ± 0.66 mmHg, similar to its baseline IOP, whereas the free-Dex group had a mean IOP of 19.38 ± 1.8 mmHg (p < 0.001) (see Fig. 6B and Table 3). Of note, neither one of the steroid treated groups had a clinically significant elevation in IOP, however the D-Dex group had a more favorable outcome with a more modest increase in IOP and no apparent IOP spike. This can be attributed to the slow steroid release profile of this particular dendrimer-dexamethasone formulation. Avoiding an IOP spike or persistent elevation in IOP is a significant advantage in clinical practice.

Estimated area of neovascularization: Neovascular vessels appeared in all groups no earlier than POD3. As shown in Figs. 6C and 7 and Table 3, the area occupied by neo-vessels remained relatively stable in the D-Dex group with a mean area of 2.5 ± 0.32 mm^2 at POD7; for comparison the mean area in the free-Dex group was 3.32 ± 0.34 (p = 0.009). Neovascularization is a later sequela in the inflammatory cascade. Inhibition of inflammation at earlier stages could explain the difference seen here, with D-Dex having the best outcome.

Corneal opacity score: Median opacity scores were all zero at baseline for all studied groups. The corneas lost their transparency as soon as POD1, however, the positive control group never recovered, as shown in Figs. 6D and 7 and Table 3– at POD14 the control group had a mean opacity score of 2.5 (range: 1–4). Statistically significant differences were observed between the groups as soon as POD3: the median opacity score for the D-Dex group was 2.5 (range: 0–4) whereas for the free-Dex group it was 3.5 (range:1–3, p < 0.001). This difference remained statistically significant at POD7 (p = 0.006) and at POD14 (p = 0.008). Corneal opacity in the constellation of alkali burn is a result of corneal inflammation and edema. The D-Dex group had the best outcome in terms of clinically-relevant assessed corneal opacity (see Figs. 6D and 7 and Table 3). This is another measure of the enhanced efficacy of the D-Dex conjugate in the treatment of corneal inflammation.

3.10.2. Biochemical parameters

Immunohistochemistry and confocal microscopy: We used immunohistochemistry and high resolution imaging using confocal microscopy at POD 7 and 14 in order to qualitatively assess the number of macrophages present in the central cornea. This measure provided an additional indirect estimate of the ability of the different treatments to decrease tissue inflammation. As previously explained in the biodistribution section, alkali burns cause structural damage and macrophage infiltration of the cornea.

The positive control group, that was treated with a placebo gel showed accumulation of macrophages in the central cornea at POD7, similar to what was seen in corneas exposed to alkali burn that had not been given any steroid treatment whatsoever. A persistent Iba-1 positive infiltrate (macrophages) was observed at POD 14 in these positive controls. We also observed some improvement in central corneal architecture that can be attributed to the natural healing process in rat model (Fig. 8 right panel). The Free-Dex gel group also demonstrated an Iba-1 positive cellular infiltrate (macrophages) of the central corneas at POD7, however it did partially resolve by POD14, this can be attributed to the therapeutic activity of free-Dex released from the subconjunctival gel (Fig. 8 middle panel). The best results in terms of macrophage depletion were seen in the D-Dex group, in which the lowest number of infiltrating cells was identified at POD7. By POD14, that infiltrate had almost completely resolved (Fig. 8 left panel).

3.10.3. Evaluation of inflammatory cytokine production using RT-PCR—In order to further characterize the response to treatment in terms of amelioration of inflammation, inflammatory cytokines were assessed at POD7 and POD14. It is widely reported that alkali burn results in elevation of inflammatory cytokines (TNF-α, IL-1β, IL-6, IL-8 and VEGF) both in acute and chronic phases [7,57]. At POD7, IL-6 mRNA levels were significantly lower in the D-Dex group when compared to positive controls (mean ± SEM 0.7 ± 0.13 vs. 9.8 ± 3.53, $p < 0.001$) (Fig. 9); this was also true for the comparison of IL-6 levels in the free-Dex group compared to the positive controls (3.0 ± 0.3 vs. 9.8 ± 3.53, $p < 0.001$). MCP-1 mRNA levels were significantly lower at POD7 in the D-Dex group compared to the positive controls (0.7 ± 0.13 vs 4.0 ± 1.24, $p < 0.001$); however, this was not true for the comparison of the free-Dex group to the positive controls ($p = 0.259$) (Fig. 9). At POD14, both D-Dex and free-Dex group had benefited from treatment in comparison to the positive controls, as shown by the mRNA levels of MCP-1: 12.5 ± 5.49 and 15.4 ± 3.22, respectively vs. 98.7 ± 15.42 in the positive control group ($p < 0.001$ for both comparisons). Of note, at POD14 the mRNA levels of VEGF were only significantly lower in the D-Dex group when compared to the positive controls (6.3 ± 1.02 vs. 27.2 ± 5.66, $p < 0.001$; $p = 0.004$ for the comparison between free-Dex and the positive controls) (Fig. 9). This difference in mRNA for VEGF may explain why the D-Dex group had less corneal neovascularization at POD14 compared to the other groups. Overall, the results of the cytokine analysis are consistent with the clinically-relevant results of the study suggesting that the D-Dex group had the best outcome in terms of corneal inflammation resolution. This anti-inflammatory activity is highly beneficial in reducing the chances of graft failure in corneal transplantation surgeries.

4. Conclusions

Corneal inflammation is an important pathological event implicated to play a crucial role in many diseases progressing to their advance stages by disrupting normal corneal homeostasis. Topical steroids are beneficial in reducing leukocyte/macrophage recruitment but required to be dosed frequently which may result in corneal toxicity and melting [58–60]. Therapies aimed at targeting the very cells responsible for inflammation and delivering steroids in a sustained manner, which can be administered at the time of surgery may be a viable option. In this study, we used mild rat alkali burn injury as a model for corneal inflammation. The

intrinsic targeting ability of PAMAM G4 hydroxyl dendrimers to localize in activated corneal macrophages is utilized to develop a sustained, targeted and intracellular delivery of dexamethasone to attenuate corneal inflammation. The highly soluble conjugates demonstrated improved anti-inflammatory activity (~1.6 fold at 10-fold lower concentration than that of free dexamethasone) in LPS activated macrophages *in vitro*. To extend and sustain the bioavailability of D-Dex, we developed an injectable gel system based on dendrimer and hyaluronic acid, crosslinked thiol-ene click photo chemistry. The gel formulations possess viscoelastic properties, are easily injectable and provide a sustained release of D-Dex. The dendrimers released from the injectable gel after subconjunctival administration targets and co-localizes in activated macrophages in central cornea with alkali burn. A single subconjunctival injection of D-Dex incorporated gel lead to prolonged efficacy for a period of 2 weeks. The D-Dex gel treatment demonstrated better outcomes such as reduced central corneal thickness, improved corneal clarity with no signs of elevation of intraocular pressure. The pharmacodynamics effect of D-Dex gel treatment attenuating corneal inflammation was demonstrated by significant reduction in macrophage infiltration in to central cornea and suppressed pro-inflammatory cytokines production compared to free drug.

The is study supports the initial hypothesis that dendrimers are effective treatment vehicles in inflammatory disorders of the cornea. This study is also unique in the route of administration for the dendrimer-gel formulation– subconjunctival. This route is clinically accessible, does not necessitate an expensive resource such as an operating room, and the potential space can allow the administration of a relatively large volume of a drug. The subconjunctival administration of a drug reservoir at the time of treatment frees the patient of the need for repeat instillation of a topical drop and may improve compliance and outcome. Despite of the recent development of depot drugs for the posterior segment of the eye, to date there is no commercially available drug specifically designed to provide long standing drug delivery to the cornea. The system depicted in this study is specifically designed to deliver drugs to the anterior segment of the eye and has been shown to be efficacious in treating corneal inflammation in this study.

Supplementary Material

Refer to Web version on PubMed Central for supplementary material.

Acknowledgments

This study was supported by the funds from KKESH-Wilmer collaborative funds, Kwok cornea research funds, and NEI RO1 EY025304(RMK). The authors also thank Wilmer Core Module for Microscopy and Imaging for allowing us to use LSM710 confocal. We also thank the Johns Hopkins University School of Medicine (SOM) Institute for Basic Biomedical Sciences (IBBS) Microscope Facility for SEM studies.

Appendix A. Supplementary data

Supplementary data related to this article can be found at http://dx.doi.org/10.1016/j.biomaterials.2017.02.016.

References

1. Stevenson W, Chauhan SK, Dana R. Dry eye disease: an immune-mediated ocular surface disorder. Arch Ophthalmol. 2012; 130(1):90–100. [PubMed: 22232476]
2. Guo H, Gao J, Wu X. Toll-like receptor 2 siRNA suppresses corneal inflammation and attenuates Aspergillus fumigatus keratitis in rats. Immunol Cell Biol. 2012; 90(3):352–357. [PubMed: 21647173]
3. Ke Y, Wu Y, Cui X, Liu X, Yu M, Yang C, Li X. Polysaccharide hydrogel combined with mesenchymal stem cells promotes the healing ofcorneal alkali burn in rats. PloS One. 2015; 10(3):e0119725. [PubMed: 25789487]
4. Weber M, Kodjikian L, Kruse FE, Zagorski Z, Allaire CM. Efficacy and safety of indomethacin 0.1% eye drops compared with ketorolac 0.5% eye drops in the management of ocular inflammation after cataract surgery. Acta Ophthalmol. 2013; 91(1):e15–e21. [PubMed: 22970738]
5. Oh JY, Lee RH, Yu JM, Ko JH, Lee HJ, Ko AY, Roddy GW, Prockop DJ. Intravenous mesenchymal stem cells prevented rejection of allogeneic corneal transplants by aborting the early inflammatory response. Mol Ther. 2012; 20(11):2143–2152. [PubMed: 22929658]
6. Tal K, Strassmann E, Loya N, Ravid A, Kariv N, Weinberger D, Katzir A, Gaton DD. Corneal cut closure using temperature-controlled CO2 laser soldering system. Lasers Med Sci. 2015; 30(4): 1367–1371. [PubMed: 25796630]
7. Javorkova E, Trosan P, Zajicova A, Krulova M, Hajkova M, Holan V. Modulation of the early inflammatory microenvironment in the alkali-burned eye by systemically administered interferon-γ-treated mesenchymal stromal cells. Stem cells Dev. 2014; 23(20):2490–2500. [PubMed: 24849741]
8. Sari ES, Yazici A, Aksit H, Yay A, Sahin G, Yildiz O, Ermis SS, Seyrek K, Yalcin B. Inhibitory effect of sub-conjunctival Tocilizumab on alkali burn induced corneal neovascularization in rats. Curr Eye Res. 2015; 40(1):48–55. [PubMed: 24910898]
9. Comstock TL, DeCory HH. Advances in corticosteroid therapy for ocular inflammation: loteprednol etabonate. Int J Inflamm. 2012; 2012
10. Stewart R, Horwitz B, Howes J, Novack GD, Hart K. Double-masked, placebo-controlled evaluation of loteprednol etabonate 0.5 for postoperative inflammation. J Cataract Refract Surg. 1998; 24(11):1480–1489. [PubMed: 9818338]
11. Kambhampati SP, Kannan RM. Dendrimer nanoparticles for ocular drug delivery. J Ocular Pharmacol Ther. 2013; 29(2):151–165.
12. Xu Q, Kambhampati SP, Kannan RM. Nanotechnology approaches for ocular drug delivery. Middle East Afr J Ophthalmol. 2013; 20(1):26. [PubMed: 23580849]
13. Lee JS, Kim YH, Park YM. The toxicity of nonsteroidal anti-inflammatory eye drops against human corneal epithelial cells in vitro. J Korean Med Sci. 2015; 30(12):1856–1864. [PubMed: 26713063]
14. Hedayatfar A, Hashemi H, Asgari S, Chee SP. Comparison of efficacy and ocular surface toxicity of topical preservative-free methylprednisolone and preserved prednisolone in the treatment of acute anterior uveitis. Cornea. 2014; 33(4):366–372. [PubMed: 24351572]
15. Skalka HW, Prchal JT. Effect of corticosteroids on cataract formation. Arch Ophthalmol. 1980; 98(10):1773–1777. [PubMed: 7425901]
16. Pleyer U, Ursell PG, Rama P. Intraocular pressure effects of common topical steroids for post-cataract inflammation: are they all the same? Ophthalmol Ther. 2013; 2(2):55–72. [PubMed: 25135807]
17. Merkoudis N, Wikberg Matsson A, Granstam E. Comparison of peroperative subconjunctival injection of methylprednisolone and standard postoperative steroid drops after uneventful cataract surgery. Acta Ophthalmol. 2014; 92(7):623–628. [PubMed: 24479722]
18. Pan Q, Xu Q, Boylan NJ, Lamb NW, Emmert DG, Yang JC, Tang L, Heflin T, Alwadani S, Eberhart CG. Corticosteroid-loaded biodegradable nanoparticles for prevention of corneal allograft rejection in rats. J Control Release. 2015; 201:32–40. [PubMed: 25576786]
19. McCartney H, Drysdale I, Gornall A, Basu P. An autoradiographic study of the penetration of subconjunctivally injected hydrocortisone into the normal and inflamed rabbit eye. Invest Ophthalmol Vis Sci. 1965; 4(3):297–302.

20. Athanasiadis Y, Tsatsos M, Sharma A, Hossain P. Subconjunctival triamcinolone acetonide in the management of ocular inflammatory disease. J Ocular Pharmacol Therapeutics. 2013; 29(6):516–522.
21. Saud EE, Moraes HV Jr, Marculino LG, Gomes JAP, Allodi S, Miguel NC. Clinical and histopathological outcomes of subconjunctival triamcinolone injection for the treatment of acute ocular alkali burn in rabbits. Cornea. 2012; 31(2):181–187. [PubMed: 22081154]
22. Kharod-Dholakia B, Randleman JB, Bromley JG, Stulting RD. Prevention and treatment of corneal graft rejection: current practice patterns of the Cornea Society. Cornea. 2011; 34(6):609–614. 2015.
23. Kang S, Chung SK. The effect of subconjuctival combined treatment of bevacizumab and triamcinolone acetonide on corneal neovascularization in rabbits. Cornea. 2010; 29(2):192–196. [PubMed: 20098156]
24. Weijtens O, Schoemaker RC, Romijn FP, Cohen AF, Lentjes EG, van Meurs JC. Intraocular penetration and systemic absorption after topical application of dexamethasone disodium phosphate. Ophthalmology. 2002; 109(10):1887–1891. [PubMed: 12359610]
25. Weijtens O, Feron EJ, Schoemaker RC, Cohen AF, Lentjes EG, Romijn FP, van Meurs JC. High concentration of dexamethasone in aqueous and vitreous after subconjunctival injection. Am J Ophthalmol. 1999; 128(2):192–197. [PubMed: 10458175]
26. Chaplot SP, Rupenthal ID. Dendrimers for gene delivery–a potential approach for ocular therapy? J Pharm Pharmacol. 2014; 66(4):542–556. [PubMed: 24635556]
27. Nance E, Zhang F, Mishra MK, Zhang Z, Kambhampati SP, Kannan RM, Kannan S. Nanoscale effects in dendrimer-mediated targeting of neuroinflammation. Biomaterials. 2016; 101:96–107. [PubMed: 27267631]
28. Patil ML, Zhang M, Taratula O, Garbuzenko OB, He H, Minko T. Internally cationic polyamidoamine PAMAM-OH dendrimers for siRNA delivery: effect of the degree of quaternization and cancer targeting. Biomacromolecules. 2009; 10(2):258–266. [PubMed: 19159248]
29. Menjoge AR, Kannan RM, Tomalia DA. Dendrimer-based drug and imaging conjugates: design considerations for nanomedical applications. Drug Discovery Today. 2010; 15(5–6):171–185. [PubMed: 20116448]
30. Sk UH, Kambhampati SP, Mishra MK, Lesniak WG, Zhang F, Kannan RM. Enhancing the efficacy of Ara-C through conjugation with PAMAM dendrimer and linear PEG: a comparative study. Biomacromolecules. 2013; 14(3):801–810. [PubMed: 23373724]
31. Kannan S, Dai H, Navath RS, Balakrishnan B, Jyoti A, Janisse J, Romero R, Kannan RM. Dendrimer-based postnatal therapy for neuroinflammation and cerebral palsy in a rabbit model. Sci Transl Med. 2012; 4(130):130ra46–130ra46.
32. Kambhampati SP, Mishra MK, Mastorakos P, Oh Y, Lutty GA, Kannan RM. Intracellular delivery of dendrimer triamcinolone acetonide conjugates into microglial and human retinal pigment epithelial cells. Eur J Pharm Biopharm. 2015; 95:239–249. [PubMed: 25701805]
33. Iezzi R, Guru BR, Glybina IV, Mishra MK, Kennedy A, Kannan RM. Den-drimer-based targeted intravitreal therapy for sustained attenuation of neuroinflammation in retinal degeneration. Biomaterials. 2012; 33(3):979–988. [PubMed: 22048009]
34. Kambhampati SP, Clunies-Ross AJ, Bhutto I, Mishra MK, Edwards M, McLeod DS, Kannan RM, Lutty G. Systemic and intravitreal delivery of dendrimers to activated microglia/macrophage in ischemia/reperfusion mouse RetinaRetinal microglia uptake of dendrimers. Invest Ophthalmol Vis Sci. 2015; 56(8):4413–4424. [PubMed: 26193917]
35. Lesniak WG, Mishra MK, Jyoti A, Balakrishnan B, Zhang F, Nance E, Romero R, Kannan S, Kannan RM. Biodistribution of fluorescently labeled PAMAM dendrimers in neonatal rabbits: effect of neuroinflammation. Mol Pharm. 2013; 10(12):4560–4571. [PubMed: 24116950]
36. Mishra MK, Beaty CA, Lesniak WG, Kambhampati SP, Zhang F, Wilson MA, Blue ME, Troncoso JC, Kannan S, Johnston MV. Dendrimer brain uptake and targeted therapy for brain injury in a large animal model of hypothermic circulatory arrest. ACS nano. 2014; 8(3):2134–2147. [PubMed: 24499315]

37. Vandamme TF, Brobeck L. Poly (amidoamine) dendrimers as ophthalmic vehicles for ocular delivery of pilocarpine nitrate and tropicamide. J Control Release. 2005; 102(1):23–38. [PubMed: 15653131]
38. Boddu SH, Jwala J, Vaishya R, Earla R, Karla PK, Pal D, Mitra AK. Novel nanoparticulate gel formulations of steroids for the treatment of macular edema. J Ocular Pharmacol Ther. 2010; 26(1):37–48.
39. Rieke ER, Amaral J, Becerra SP, Lutz RJ. Sustained subconjunctival protein delivery using a thermosetting gel delivery system. J Ocular Pharmacol Ther. 2010; 26(1):55–64.
40. Sharma R, Kottari N, Chabre YM, Abbassi L, Shiao TC, Roy R. A highly versatile convergent/divergent “onion peel” synthetic strategy toward potent multivalent glycodendrimers. Chem Commun. 2014; 50(87):13300–13303.
41. Lutty GA, Merges C, Threlkeld AB, Crone S, McLeod DS. Heterogeneity in localization of isoforms of TGF-beta in human retina, vitreous, and choroid, Invest. Ophthalmol Vis Sci. 1993; 34(3):477–487.
42. Larkin D, Calder V, Lightman S. Identification and characterization of cells infiltrating the graft and aqueous humour in rat corneal allograft rejection. Clin Exp Immunol. 1997; 107(2):381–391. [PubMed: 9030879]
43. Thygesen J, Jensen O. pH changes of the tear fluid in the conjunctival sac during postoperative inflammation of the human eye. Acta Ophthalmol. 1987; 65(2):134–136. [PubMed: 3604601]
44. Macky TA, Oelkers C, Rix U, Heredia ML, Künzel E, Wimberly M, Rohrer B, Crosson CE, Rohr J. Synthesis, pharmacokinetics, efficacy, and rat retinal toxicity of a novel mitomycin C-triamcinolone acetonide conjugate. J Med Chem. 2002; 45(5):1122–1127. [PubMed: 11855992]
45. Kafedjiiski K, Jetti RK, Föger F, Hoyer H, Werle M, Hoffer M, Bernkop-Schnürch A. Synthesis and in vitro evaluation of thiolated hyaluronic acid for mucoadhesive drug delivery. Int J Pharm. 2007; 343(1):48–58. [PubMed: 17544606]
46. Shu XZ, Liu Y, Luo Y, Roberts MC, Prestwich GD. Disulfide cross-linked hyaluronan hydrogels. Biomacromolecules. 2002; 3(6):1304–1311. [PubMed: 12425669]
47. Oh EJ, Park K, Kim KS, Kim J, Yang JA, Kong JH, Lee MY, Hoffman AS, Hahn SK. Target specific and long-acting delivery of protein, peptide, and nucleotide therapeutics using hyaluronic acid derivatives. J Control Release. 2010; 141(1):2–12. [PubMed: 19758573]
48. Schanté CE, Zuber G, Herlin C, Vandamme TF. Chemical modifications of hyaluronic acid for the synthesis of derivatives for a broad range of biomedical applications. Carbohydr Polym. 2011; 85(3):469–489.
49. Oudshoorn MH, Rissmann R, Bouwstra JA, Hennink WE. Synthesis of methacrylated hyaluronic acid with tailored degree of substitution. Polymer. 2007; 48(7):1915–1920.
50. Gramlich WM, Kim IL, Burdick JA. Synthesis and orthogonal photo-patterning of hyaluronic acid hydrogels with thiol-norbornene chemistry. Biomaterials. 2013; 34(38):9803–9811. [PubMed: 24060422]
51. Aimetti AA, Machen AJ, Anseth KS. Poly (ethylene glycol) hydrogels formed by thiol-ene photopolymerization for enzyme-responsive protein delivery. Biomaterials. 2009; 30(30):6048–6054. [PubMed: 19674784]
52. Fairbanks BD, Schwartz MP, Halevi AE, Nuttelman CR, Bowman CN, Anseth KS. A versatile synthetic extracellular matrix mimic via thiol-norbornene photopolymerization. Adv Mater. 2009; 21(48):5005–5010. [PubMed: 25377720]
53. Sharma R, Zhang I, Shiao TC, Pavan GM, Maysinger D, Roy R. Low generation polyamine dendrimers bearing flexible tetraethylene glycol as nanocarriers for plasmids and siRNA. Nanoscale. 2016; 8(9):5106–5119. [PubMed: 26868181]
54. Silver FH, LiBrizzi J, Pins G, Wang MC, Benedetto D. Physical properties of hyaluronic acid and hydroxypropylmethylcellulose in solution: evaluation of coating ability. J Appl Biomater. 1994; 5(1):89–98.
55. Jafari MR, Markwardt KL, Doshi U. Combinations of viscoelastics for use during surgery. Google Patents. 2013

56. Calciu-Rusu D, Rothfuss E, Eckelt J, Haase T, Dick HB, Wolf BA. Rheology of sodium hyaluronate saline solutions for ophthalmic use. Biomacromolecules. 2007; 8(4):1287–1292. [PubMed: 17355119]

57. Planck S, Rich L, Ansel J, Huang X, Rosenbaum J. Trauma and alkali burns induce distinct patterns of cytokine gene expression in the rat cornea. Ocular Immunol Inflamm. 1997; 5(2):95–100.

58. Wagoner MD. Chemical injuries of the eye: current concepts in pathophysiology and therapy. Surv Ophthalmol. 1997; 41(4):275–313. [PubMed: 9104767]

59. Den S, Sotozono C, Kinoshita S, Ikeda T. Efficacy of early systemic betamethasone or cyclosporin A after corneal alkali injury via inflammatory cytokine reduction. Acta Ophthalmol Scand. 2004; 82(2):195–199. [PubMed: 15043540]

60. Donshik PC, Berman MB, Dohlman CH, Gage J, Rose J. EFfect of topical corticosteroids on ulceration in alkali-burned corneas. Arch Ophthalmol. 1978; 96(11):2117–2120. [PubMed: 214063]

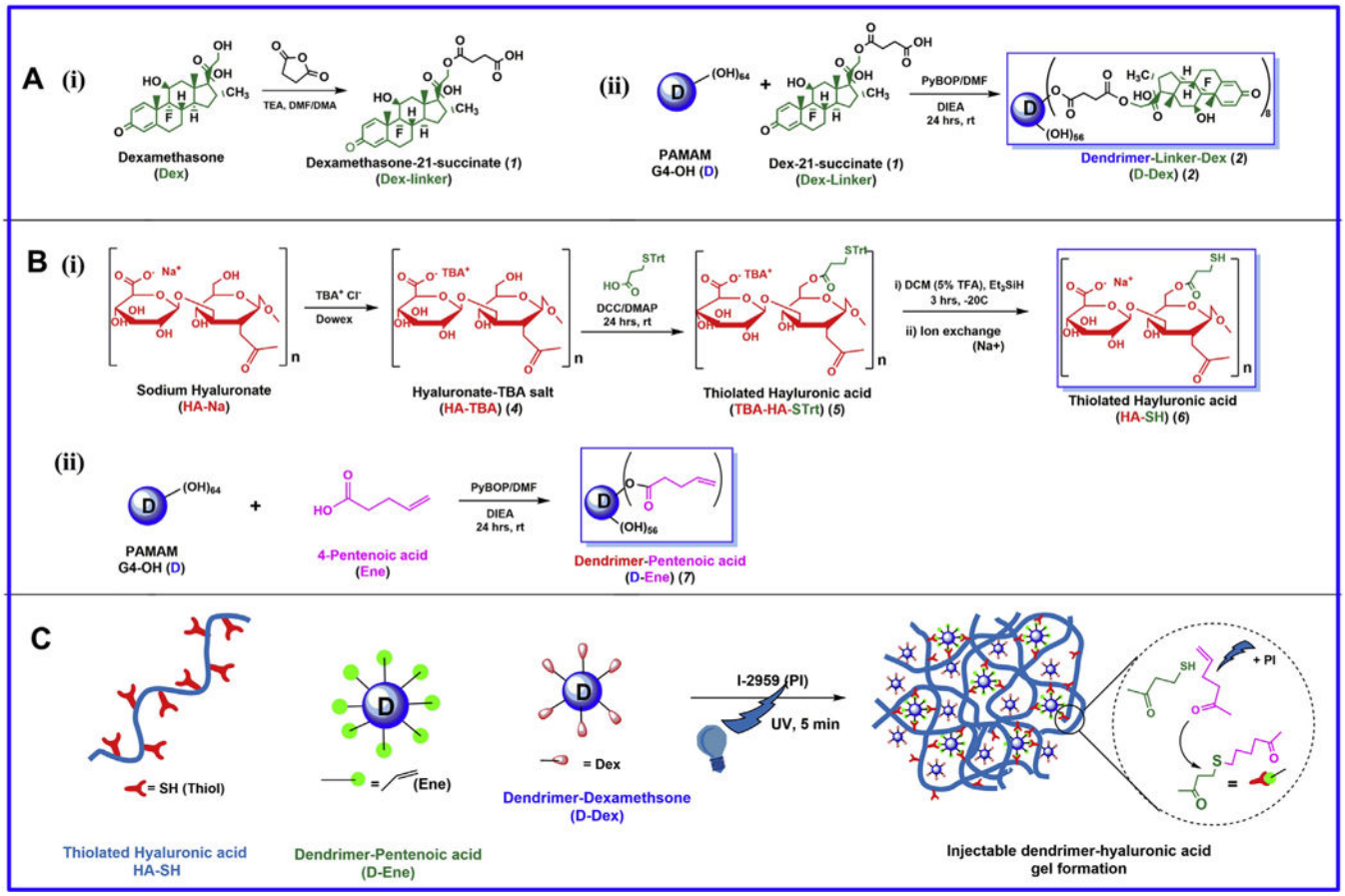

Fig. 1. Preparation of dendrimer conjugates and injectable gel components

A) Synthesis of dendrimer dexamethasone conjugates (D-Dex). **B)** Synthesis of individual components of the injectable gel **(i)** Thiolated Hyaluronic acid (HA-SH) and **(ii)** dendrimer-Pentenoic acid (D-Ene) conjugates. **C)** A schematic representation of formation of D-Dex loaded injectable gel by thiol-ene click chemistry.

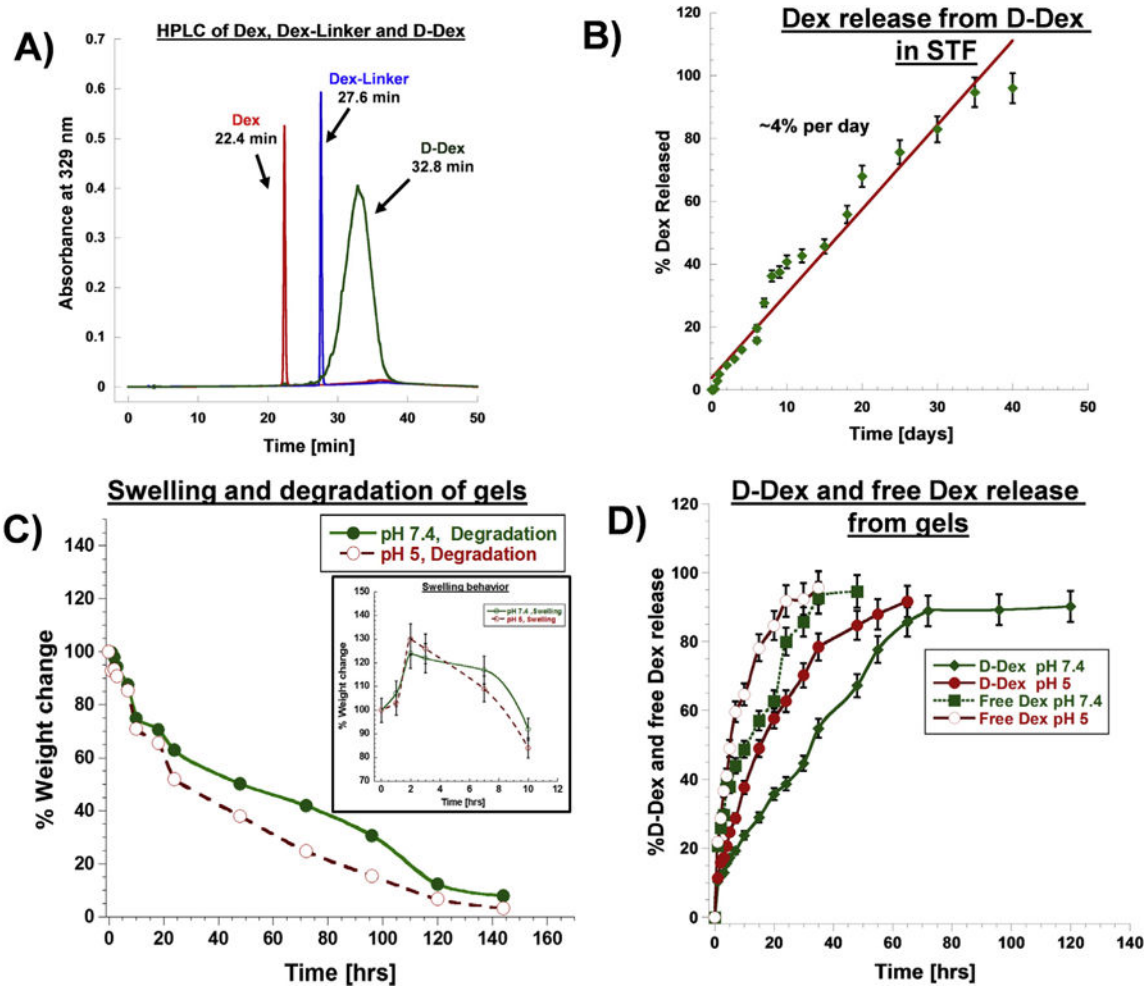

Fig. 2. Characterization of prepared conjugates

A) HPLC chromatograms of D-Dex (32.8 min), Dex (22.4 min) and Dex-Linker (27.6 min) monitored at 239 nm. **B)** Drug release profile from D-Dex conjugates in simulated tear fluid. **C)** Swelling and degradation profile of injectable gel in pH 7.4 and 5 respectively, **inset** – weight change measurements depicting the swelling behavior of the gel. **D)** D-Dex and Free Dex release profile from injectable gel formulations in pH 7.4 and 5 respectively.

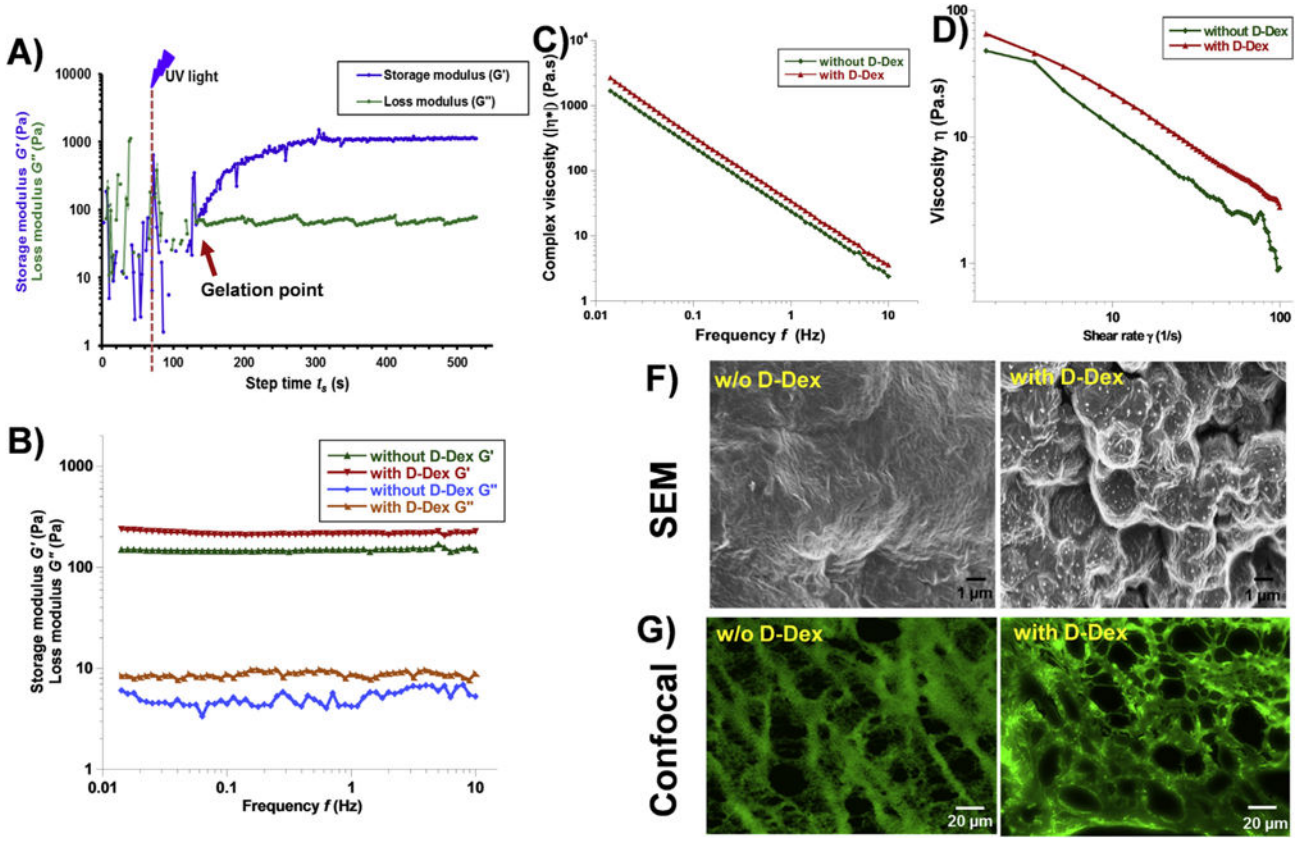

Fig. 3. Characterization of injectable gels using rheology and SEM

A) Dynamic time sweep photo-rheology of injectable gel formation. The gelation point is approximated when storage modulus (G′) overcomes the loss modulus (G″) (arrow). Dashed line (–) illustrates when the UV light was turned on. **B**) Frequency sweep measurements of the injectable gel demonstrating their viscoelastic behavior (G′ ⩾ G″). **C)** viscosity vs frequency plot of injectable gel with and without D-Dex showing similar dynamic viscosity. **D**) Viscosity vas shear rate plots of injectable gels with and w/o D-Dex showing shear thinning properties. **F)** SEM images of dehydrated injectable gels with and without D-Dex showing the surface morphology. **G**) Confocal images of the FITC stained gel sections demonstrating the inner morphology with porous structure.

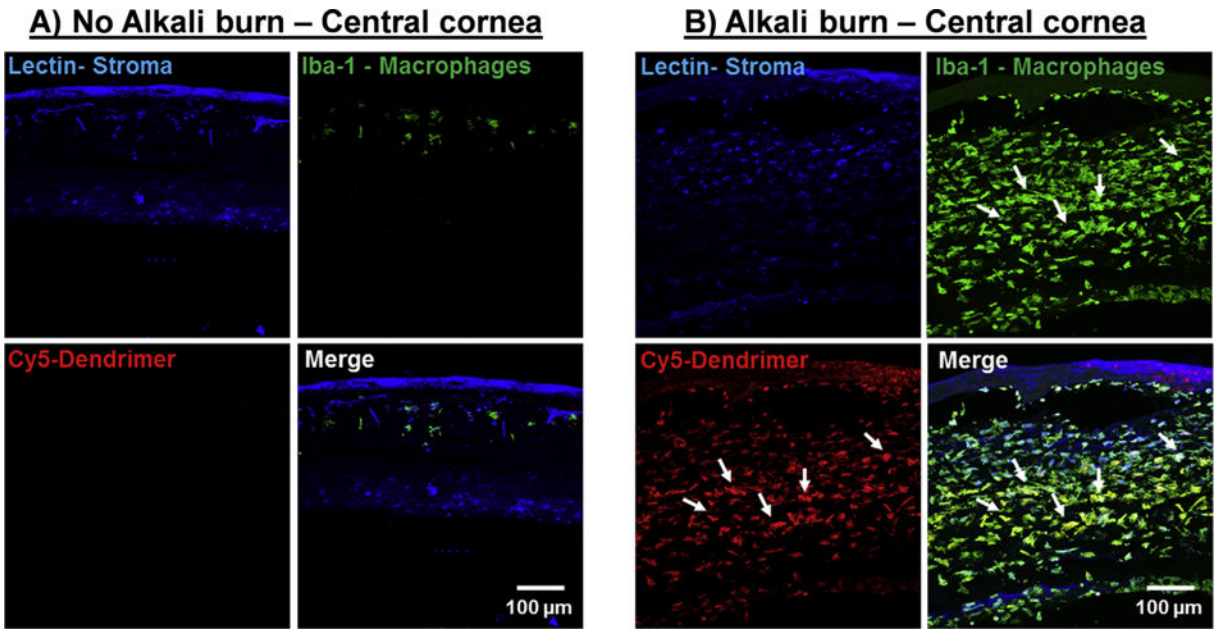

Fig. 4. Biodistribution of subconjunctivally injected dendrimers

Fluorescently labelled dendrimers (D-Cy5) in gel formulations were injected subconjuntivally and the biodistribution was assessed 7 days after injection. Corneal stroma (Blue, Lectin), Macrophages (Green, Iba-1), Dendrimer (Red, Cy5). **A)** A central cross section of a normal cornea with regular tissue architecture; very few corneal Iba-1 stained cells (macrophages) are present; dendrimers are not co-localized in the macrophages. **B)** An alkali burnt central cornea infiltrated with Iba-1 positive cells (macrophages). Cy5 signals (dendrimer) are co-localized in the Iba-1 stained cells demonstrating dendrimer's intrinsic targeting capability towards inflammation. Scale bar 100 µm. (For interpretation of the references to colour in this figure legend, the reader is referred to the web version of this article.)

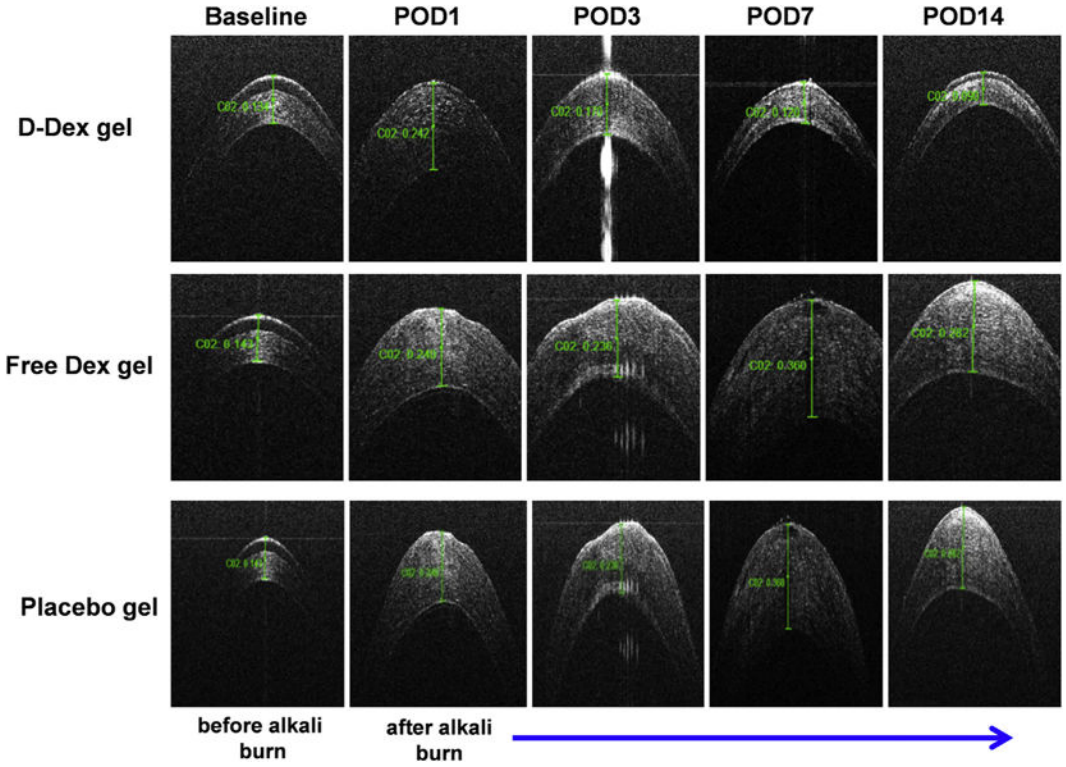

Fig. 5. Anterior segment optical coherence tomography (OCT) imaging of the cornea for assessment of central corneal thickness (CCT)

Top panel: OCT images of the central cornea of a D-Dex gel treated eye demonstrate near-normal corneal architecture at POD 7 and 14 when compared to its baseline. These images suggest that inflammation has subsided. **Middle panel:** OCT images of a central cornea treated with free-Dex gel demonstrate a thin irregular epithelial layer and stromal edema which suggest ongoing inflammation. **Bottom panel:** OCT images of a central cornea treated with placebo gel has similar characteristics as the free-Dex treated eye.

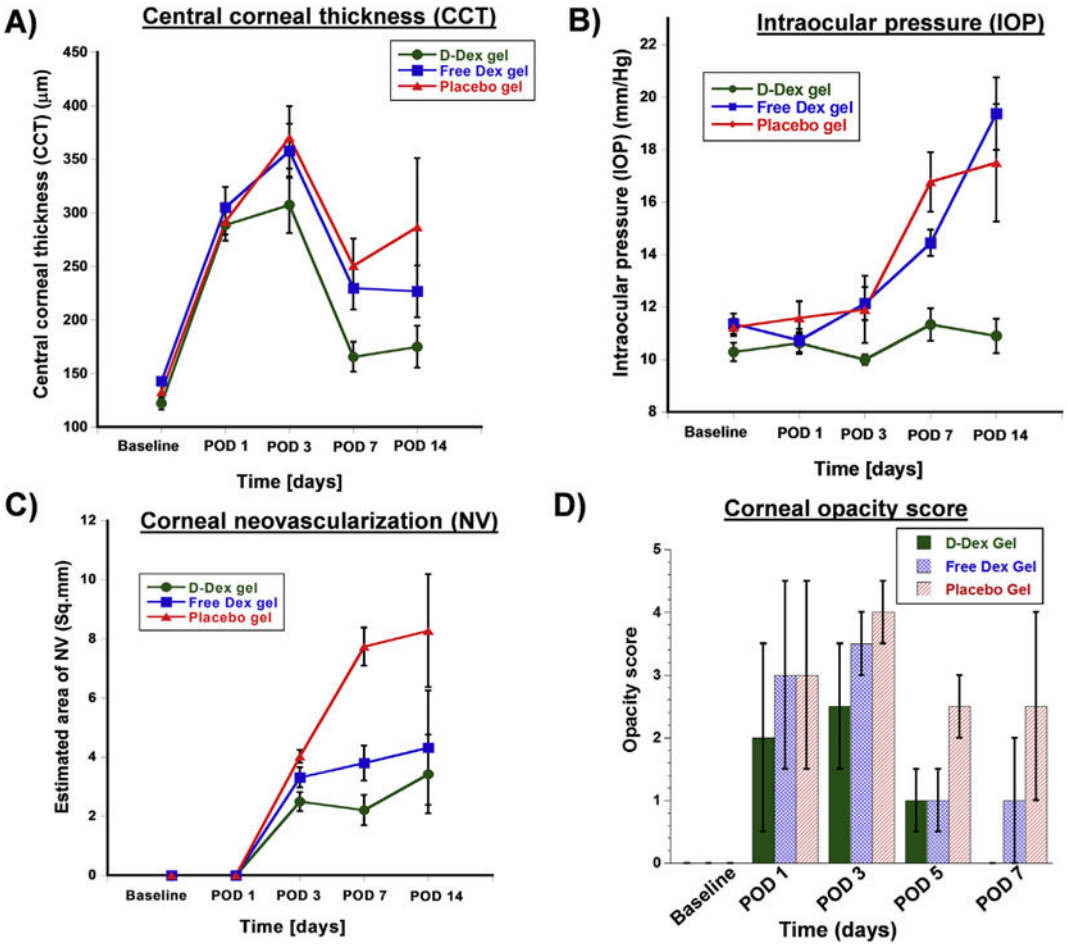

Fig. 6. Assessment of efficacy of subconjunctival gel treatment by representing the parameters as clinical scores

A) Central corneal thickness (CCT) measurements obtained by optical coherence tomography. All groups had an initial increase in CCT due to the alkali burn, however the D-Dex group gel group (the green line) had the best outcome with the lowest CCT. **B) Intraocular pressure (IOP)** measurements demonstrate a relatively stable IOP in the D-Dex gel group, whereas the free-Dex gel group and the positive controls have a gradual increase in IOP over the study period. **C) Qualitative estimated area of neovascularization**: neovascularization was first observed at post-operative day 3, and the least amount of corneal neovascularization was observed in the D-Dex gel group. **D) Corneal opacity scores**: The median opacity score of the D-Dex gel group at post-operative day 14 is zero. (For interpretation of the references to colour in this figure legend, the reader is referred to the web version of this article.)

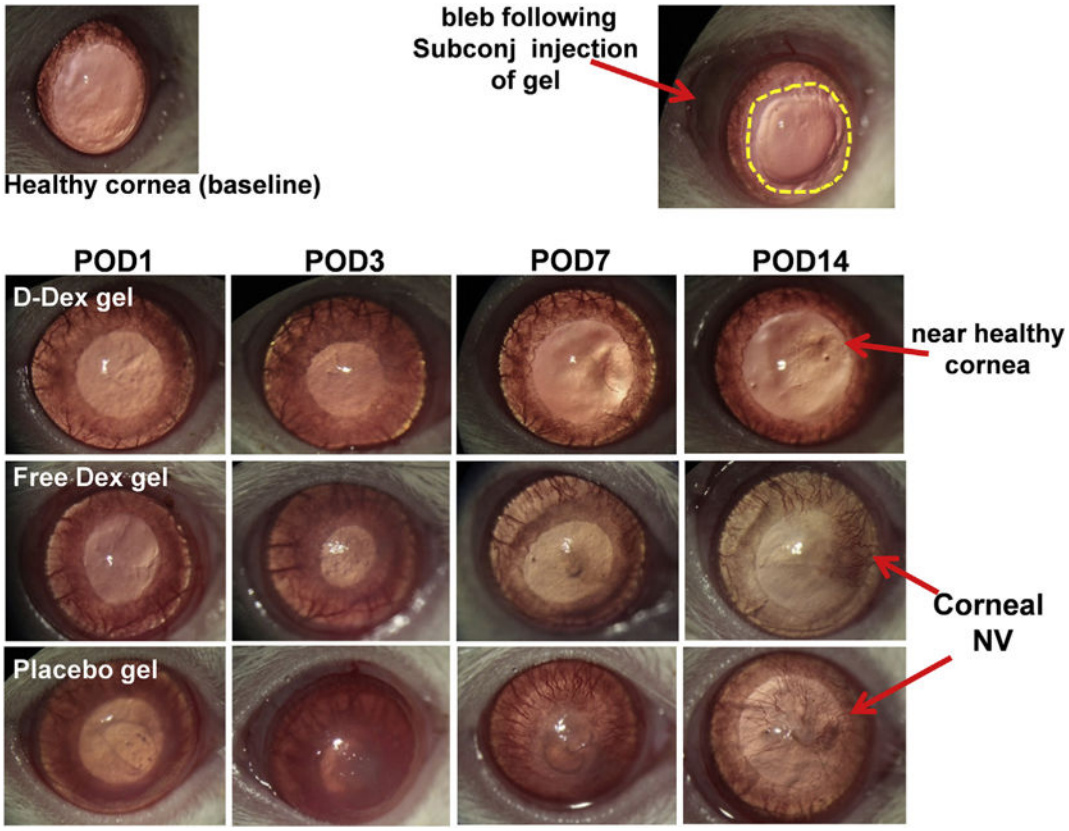

Fig. 7. Clinical assessment of efficacy of subconjunctival D-Dex and Free Dex gel for corneal opacity and neovascularization

Top left: Photograph of a healthy control: a regular iris and a clear cornea without neovascularization are depicted. **Top right:** Photograph of a rat cornea immediately after alkali burn demonstrates an epithelial defect (yellow dotted lines); a bleb (red arrow) resulted from the subconjunctival injection of D-Dex gel. **Top Panel:** Photographic images of a D-Dex gel treated eye over time. The images show a gradual decrease in corneal opacity and minimal corneal neovascularization. **Middle panel:** Free Dex gel treated group: The eye did not recover over a 14-day period with residual corneal opacity, an irregular corneal light reflex suggesting irregular epithelium and development of clinically significant corneal neovascularization. **Bottom panel:** A placebo gel treated eye shows extensive damage with a persistent epithelial defect until POD7, corneal opacity and 360° of neovascularization reaching the center of the cornea. (For interpretation of the references to colour in this figure legend, the reader is referred to the web version of this article.)

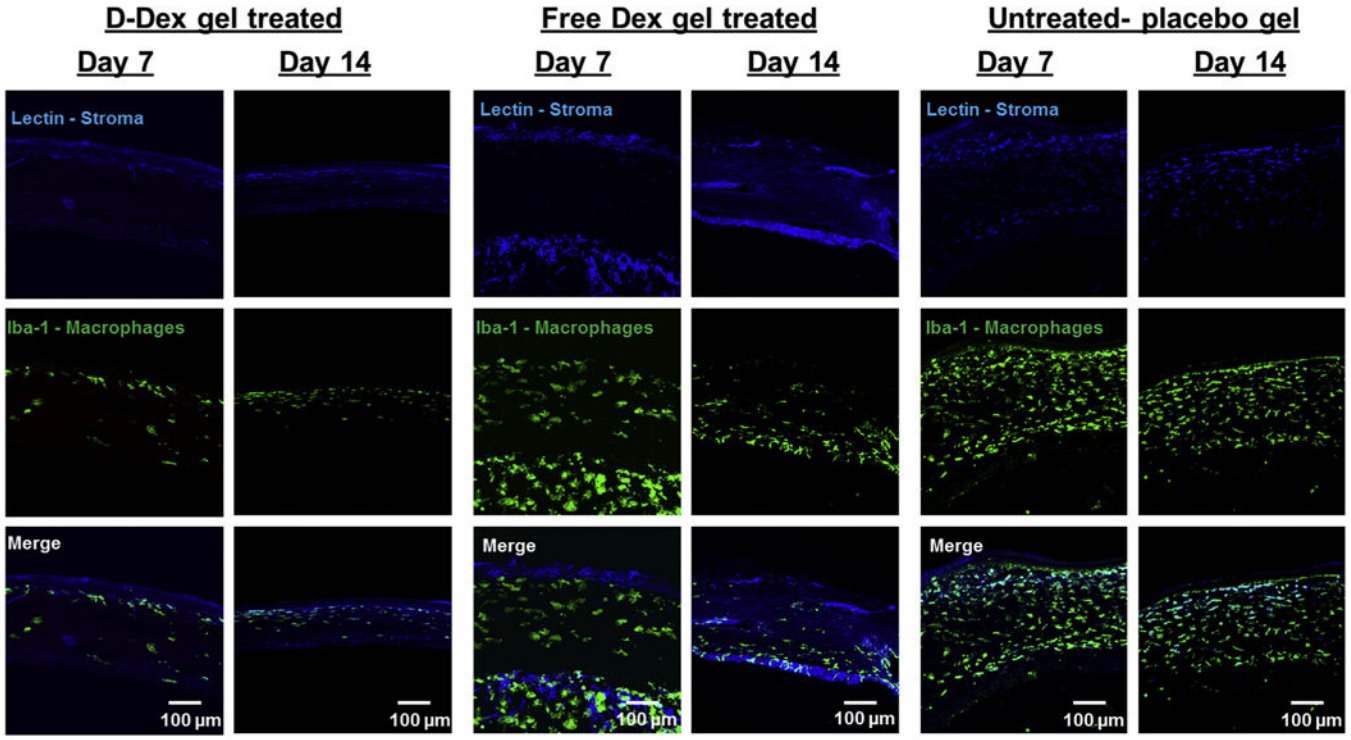

Fig. 8. Confocal microscope images of corneal cross sections

Left panel: a minimal amount of Iba-1 stained cellular infiltrate (macrophages) is observed at post-operative day 7 and 14. **Middle pane and right panels:** Unlike the D-Dex gel group, both free-Dex gel and placebo gel groups have a persistent IBA-1 stained cellular infiltrate (macrophages) at post-operative days 7 and 14. Scale bar 100 µm.

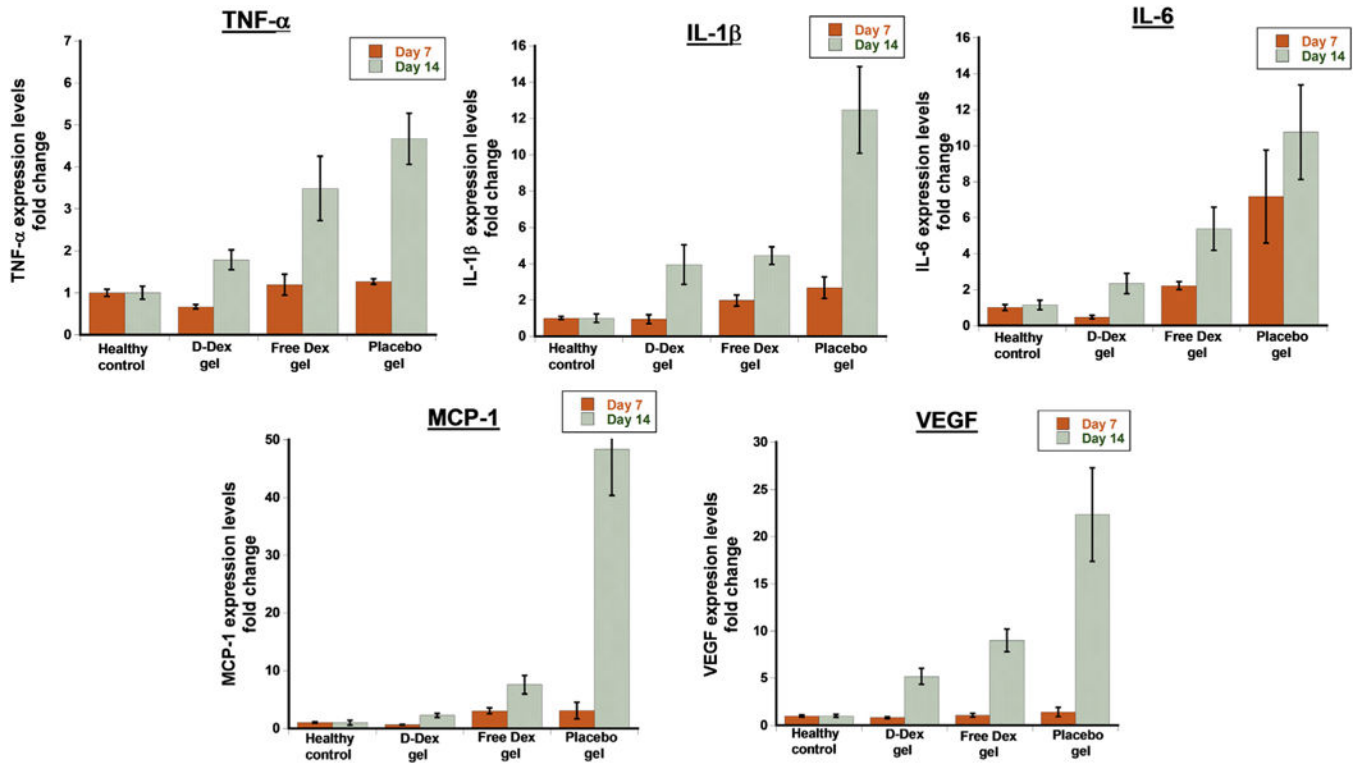

Fig. 9. Assessment of corneal inflammation after subconjunctival treatment by measuring the cytokine mRNA expression levels in corneal tissue using RT-PCR at POD 7 and 14

TNF-α – Tumor necrosis factor-**α, IL-1β** – Interleukin-1**β, IL-6** – Interleukin-6, **MCP-1** – Monocyte chemoattractant protein-1, **VEGF** – Vascular endothelial growth factor. The results are normalized to healthy controls and represented as mean ± SEM, n = 10.

Table 1

Corneal opacity scores

The degree of corneal transparency as a measure of efficacy after administration of subconjutival D-Dex, Free Dex or placebo. The grading measures were adopted from *Larkin* et al. [42].

Opacity grade	Degree of transparency
0	Transparent
1	Minimal loss of transparency
2	Iris vessels visible
3	Pupil outline visible
4	Pupil outline obscured

Table 2

Primer sequences.

Primer	Segment	Sequence
GAPDH (Glyceraldehyde 3-phosphate dehydrogenase)	Forward (5′-3′)	GCAAGAGAGAGGCCCTCA
	Reverse (3′-5′)	TGTGAGGGAGATGCTCAGTG
TNF-α (Tumor necrosis factor-α)	Forward (5′-3′)	TCAGTTCCATGGCCCAGAC
	Reverse (3′-5′)	GTTGTCTTTGAGATCCATGCCATT
IL-lβ (Interleukin-lβ)	Forward (5′-3′)	CACCTCTCAAGCAGAGCACAG
	Reverse (3′-5′)	GGGTTCCATGGTGAAGTCAAC
IL-6 (Interleukin-6)	Forward (5′-3′)	AAAGAGTTGTGCAATGGCAATTCT
	Reverse (3′-5′)	CAGTGCATCATC GCTGTTCATACA
MCP-l (monocyte chemoattractant protein −l)	Forward (5′-3′)	CTATGCAGGTCTCTGTCACGCTTC
	Reverse (3′-5′)	CAGCCGACTCATTGGGATCA
VEGF (Vascular endothelial growth factor)	Forward (5′-3′)	GGCTTTACTGCTGTACCTCC
	Reverse (3′-5′)	CAAATGCTTTCTCCGCTCT

Table 3

Summary of clinical outcomes after subconjutival treatment of D-Dex, free-Dex and placebo (Positive control) gels. All results are displayed as mean ± standard deviation except for the opacity scores that are displayed as median (inter-quartile range). POD – post operative day; CCT – central corneal thickness; NV – neovascularization; IOP –intraocular pressure.

Outcome measure	Group	Baseline	POD1	POD3	POD7	POD14
CCT (μm)	D-Dex	122.08 ± 28.17	288.58 ± 72.27	307.46 ± 128.98	165.54 ± 68.64	174.9 ± 115.15
	Free-Dex	142.86 ± 8.68	304.95 ± 87.23	357.71 ± 115.58	229.57 ± 91.54	226.57 ± 63.67
	Positive controls	132.8 ± 20.09	291.9 ± 38.67	370.3 ± 92.10	250.6 ± 79.37	286.83 ± 156.57
Opacity score	D-Dex	0(0)	2(3)	2.5(2)	1(1)	0(0)
	Free-Dex	0(0)	3(3)	3.5(1)	1(1)	1(2)
	Positive controls	0(0)	3(3)	4(1)	2.5(1)	2.5(3)
Estimated area of NV (mm^2)	D-Dex	0±0	0 ±	2.5 ± 1.57	2.21 ± 2.53	3.43 ± 4.2
	Free-Dex	0±0	0±0	3.32 ± 1.65	3.8 ± 2.89	43.32 ± 5.46
	Positive controls	0±0	0±0	4.03 ± 1.02	7.74 ± 3.02	8.29 ± 5.4
IOP (mmHg)	D-Dex	10.29 ± 1.73	10.63 ± 2.02	10.00 ± 0.98	11.33 ± 3.03	10.90±2.08
	Free-Dex	11.36 ± 1.84	10.73 ± 2.07	12.14 ± 2.93	14.45 ± 2.32	19.38±3.89
	Positive controls	11.23 ± 1.54	11.59 ± 2.97	11.91 ± 6.02	16.77 ± 5.31	17.50±6.32